PERGAMON

Deep-Sea Research II 48 (2001) 3049–3081

DEEP-SEA RESEARCH
PART II

www.elsevier.com/locate/dsr2

Pelagic production at the Celtic Sea shelf break

Ian Joint[a,*], Roland Wollast[b], Lei Chou[b], Sonia Batten[c], Marc Elskens[d], Elaine Edwards[a], Andrew Hirst[e], Peter Burkill[a], Stephen Groom[a], Stuart Gibb[a], Axel Miller[a], David Hydes[e], Frank Dehairs[d], Avan Antia[f], Raymond Barlow[a], Andrew Rees[a], Alan Pomroy[a], Uwe Brockmann[g], Denise Cummings[a], Richard Lampitt[e], Michèle Loijens[b], Fauzi Mantoura[a], Peter Miller[a], Thomas Raabe[g], Xose Alvarez-Salgado[a,h], Claire Stelfox[a], James Woolfenden[a]

[a] *NERC Centre for Coastal and Marine Sciences, Plymouth Marine Laboratory, Prospect Place, Plymouth PL1 3DH, UK*
[b] *Laboratoire d'Océanographie Chimique et Géochimie des Eaux, Université Libre de Bruxelles, Campus de la Plaine, B-1050 Brussels, Belgium*
[c] *Sir Alister Hardy Foundation for Ocean Science, c/o Plymouth Marine Laboratory, Citadel Hill, Plymouth PL1 2PB, UK*
[d] *Dienst Analytische Scheikunde, Vrije Universiteit Brussel, Pleinlaan 2, B-1050 Brussels, Belgium*
[e] *Southampton Oceanography Centre, Empress Dock, Southampton SO14 3ZH, UK*
[f] *Institut für Meereskunde, Universität Kiel, D-24105 Kiel 1, Germany*
[g] *Institute für Biochemie and Lebensmittelchemie, Universität Hamburg, Martin-Luther King Platz 6, 20146 Hamburg, Germany*
[h] *Instituto de Investigacions Mariñas, E-36208, Vigo, Spain*

Abstract

This paper reviews the data obtained in the OMEX I Project on biological production in the surface waters of the Celtic Sea shelf break. The study focused on two regions— the Goban Spur and La Chapelle Bank. Satellite images of the Celtic Sea frequently show a region of cooler water at the shelf break, which results in the mixing of cooler, nutrient-rich waters to the sea surface. To examine the hypothesis that the Celtic Sea shelf break might be a region of enhanced production and sedimentation, observations were made at five regions. These were four sites along a transect of the Goban Spur, from the Celtic Sea shelf (water depth <200 m), through stations at water depths of 500–1000, 1500, and 3600 m; the fifth region was at La Chapelle Bank, which offered a contrasting site where the slope is steeper and influenced by canyons.

Estimates are made of seasonal production of phytoplankton, bacterioplankton, microzooplankton, and mesozooplankton. The region has a spring bloom which is of short duration at the oceanic sites and occurs earliest on the Celtic Sea shelf; phytoplankton biomass in the summer months is greatest at La Chapelle Bank. Photosynthetic pigments analyses indicate that prymnesiophytes are present throughout the year and are often the dominant group of phytoplankton; diatoms are most abundant in the spring bloom. Primary

*Corresponding author. Tel.: +44-1752-633100; fax: +44-1752-633101.
E-mail address: i.joint@pml.ac.uk (I. Joint).

PII: S0967-0645(01)00032-7

production is estimated to be ca. 160 gC m^{-2} a^{-1}, with cells <5 μm in diameter accounting for almost half of the annual primary production. New production is estimated to be equivalent to 80 g C m^{-2} a^{-1}; the *f*-ratio is generally <0.25 during the summer and autumn months, 0.7–0.8 during the spring bloom, and ca. 0.5 during the winter.

Microzooplankton biomass and herbivory were measured from April to October at the Goban Spur regions. The biomass of mesozooplankton was determined from the records of the Continuous Plankton Recorder (CPR) survey, and was used to estimate the amount of primary production removed by mesozooplankton grazing. Bacterial production is estimated to be ca. 12 g C m^{-2} a^{-1}. The sum of microzooplankton and mesozooplankton grazing and the carbon demands of bacteria were significantly lower than primary production from November through May, but heterotrophic processes were quantitatively greater than phytoplankton production from July to October. The data suggest that up to 62 g C m^{-2} a^{-1} of primary production was not grazed by micro- or mesozooplankton in the surface mixed layer, or utilised directly by bacteria. Depending on the region, up to 38% of the primary production at the Celtic Sea margin was apparently not grazed in the surface mixed layer and would be available for heterotrophic organisms in mid-water and the benthos. The estimated respiration of the heterotrophic community of the surface mixed layer estimated also suggested that between 37% and 60% of the carbon fixed by photosynthesis in the euphotic zone was not remineralised in the surface mixed layer.

Data from satellite remote sensing are used in conjunction with the experimental data to extend the seasonal coverage of the observations made in OMEX I. The archive of the coastal zone color scanner provides mean monthly values of chlorophyll concentration, and these agree well with the seasonal variation of "green colour" of the CPR survey. Primary production has been estimated from the satellite-derived chlorophyll concentrations for the period April–September and is calculated to be 90 g C m^{-2} for the 6-month period; the estimated production for the same period from in situ experiments suggests that primary production was ca. 116 g C m^{-2}. Nitrate concentrations in the surface water were correlated with sea-surface temperature, and this relationship was applied to temperature measurements from the advanced very high resolution radiometer sensor to estimate the potential nitrate concentrations over the region. The *f*-ratio was related to nitrate concentration by a simple hyperbolic function ($r^2 = 0.73$). which was applied to the images of potential nitrate concentration for the region to estimate new production based on satellite data. For the period April through September, new production was calculated to be 46 g C m^{-2} from satellite estimates of temperature, nitrate, and *f*-ratio, which compares favourably with the estimated new production of 57 g C m^{-2} by direct measurement.

1. Introduction

Shelf seas generally have higher biological activity than the adjacent ocean and are the regions of greatest fish production. Understanding the functioning of shelf seas requires information on fluxes of material and energy through the shelf sea ecosystem. Much emphasis is placed on accurate assessment of nutrient and anthropogenic contaminant inputs from rivers, but net exchange with the ocean boundary is as an important parameter, which is much more difficult to measure because of the volume of water involved. The interplay between the shelf seas and slope has been the subject of much recent study since Walsh et al. (1981) suggested that there was significant loss of organic matter originating on the continental shelf to depocentres

on the slope. The hypothesis was tested during an interdisciplinary study on the Middle Atlantic Bight, called the Shelf Edge Exchange Processes experiment—SEEP I (Walsh et al., 1988). This study gave contradictory results, which, whilst suggesting that there was export of particles to the slope region, also suggested that mineralisation on the shelf was the most important process and that there was insufficient organic carbon for transport to the slope. However, a second programme, SEEP II (Biscaye et al., 1994) concentrated on the southern end of the Middle Atlantic Bight and showed unequivocally that the slope in that region does not act as a depocentre for organic carbon generated on the shelf.

The research reported here was part of the Ocean Margin EXchange (OMEX) Project, partly funded by the European Commission in the framework of the Marine Science and Technology (MAST) programme. The aim of the project was to investigate the importance of the European Ocean Margin in terms of exchange between the ocean and shelf seas, to determine if there is enhanced production in this region, and to estimate the fraction of primary production which sediments into intermediate and deep waters. The focus of the study was the NW European Shelf Edge, specifically a region at the shelf break in the Celtic Sea.

The mid-European Shelf edge has many contrasts with the Middle Atlantic Bight. One of the most striking features of the Celtic Sea is a region of cooler water at the shelf break, which is clearly visible in satellite images (Dickson et al., 1980). This is assumed to be a consequence of an internal tide, generated at the 200-m contour, which propagates both onto the shelf and into the ocean (Pingree et al., 1986). These progressive waves result in the mixing of cooler, nutrient-rich waters to the sea surface, with the potential to enhance phytoplankton production by supplying more nutrients to the euphotic zone. If the upwelling of nutrient-rich deep waters at the continental margins does enhance primary production, this could have implications for production of the rest of the food web and might result in increased sedimentation of organic matter to deep water and the sediments.

The aim of this study is to estimate the seasonal production of phytoplankton, microzooplankton, and mesozooplankton, through the use of data on pigment concentrations, primary and new production rates, microzooplankton herbivory and mesozooplankton biomass. It examines the potential for enhanced production and sedimentation at the shelf break by comparing data obtained from the surface mixed layer at five regions studied during OMEX I, 1993–1995. These are La Chapelle Bank to the south of the region, an area representative of the Celtic Sea shelf, and three regions on the slope from the top (with water depths of 500–1000 m), the middle (water depths ca. 1500 m), and towards the bottom (water depth ca. >3000 m). Data from satellite remote sensing and other studies are also used to extend the seasonal coverage of the observations made in OMEX I, with the overall aim of evaluating the cycling of organic matter in the surface water and hence the potential export of carbon and nitrogen by sedimentation. Estimates of new production provide an indication of the potential export from the seasonal mixed layer. Finally, the results are used to calculate the likely losses of organic carbon by heterotrophic processes, hence estimating the proportion of primary production which might be available for sedimentation to deeper water. This potential carbon export forms a basis for comparison with the estimates of mid- and deep water and benthic carbon demands (van Weering et al., 1998) and with estimates obtained from sediment traps (Antia et al., 1999, 2001).

2. Methods

2.1. Study area

The region of study is the shelf break of the Celtic Sea; the locations of the four regions investigated along the Goban Spur and La Chapelle Bank are shown in Fig. 1. Stations sampled during the project have been aggregated into different regions. At the Goban Spur, these are (1) an area typical of the Celtic Sea shelf, referred to as "Shelf" stations, and including all stations sampled within the area bounded by 49–50°N, 10–10.5°W; 2) an area referred to as the "OMEX 1 site"—all stations sampled at a water depth of between 500 and 1000 m within the region bounded by 49–50°N, 11–12°W; (3) the "OMEX 2 site", bounded by 48.5–49.8°N, 12–12.7°W, where a long-term sediment trap mooring was deployed at a water depth of 1440 m; (4) the "OMEX 3 site" with any stations occupied in a water column depth >3000 m within the area 48–49.5°N, 13–16.5°W, including the site of the sediment trap mooring located at 3660 m; and (5) stations at La Chapelle Bank (47–48°N, 6–8°W). At La Chapelle Bank, the slope is steeper, and more intense vertical mixing is likely to occur; this site, therefore, offers a comparison with the Goban Spur. The southern region also is influenced by the presence of canyons that traverse the continental slope. The data used in this paper result from a number of research cruises. The dates and regions sampled are given in Table 1.

2.2. Surface mixed-layer depth

In this paper, comparisons are made between stations and between seasons; in many cases, estimates of biomass or production have been integrated from the sea surface to the seasonal

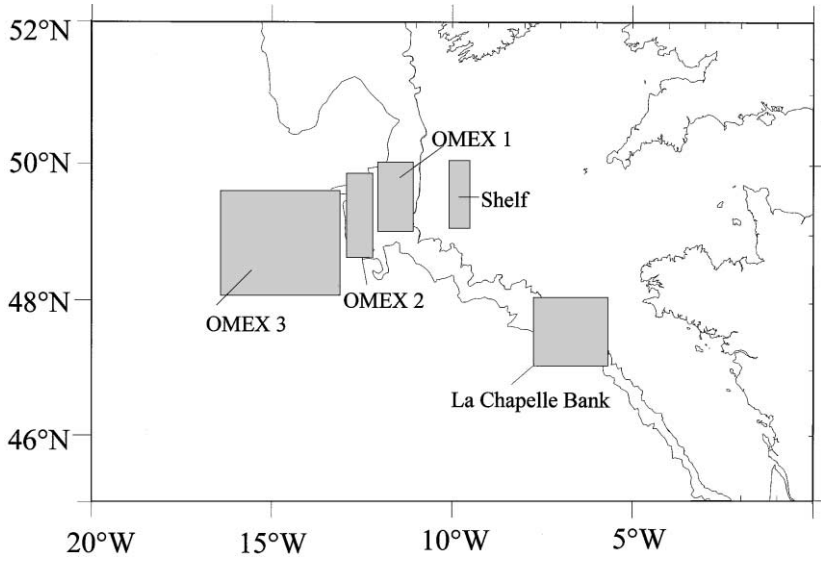

Fig. 1. The area of study at the shelf margin of the Celtic Sea; four regions of the Goban Spur are identified as Shelf, OMEX 1, OMEX 2, OMEX 3 and a fifth region is shown at La Chapelle Bank.

Table 1
Dates and regions sampled

Date	Research vessel	Regions sampled
April 1993	*Belgica*	La Chapelle Bank
June/July 1993	*Valdivia*	Goban Spur
September 1993	*Belgica*	Goban Spur, La Chapelle Bank
October 1993	*Pelagia*	Goban Spur
January 1994	*Meteor*	Goban Spur, La Chapelle Bank
January 1994	*Charles Darwin*	Goban Spur, La Chapelle Bank
April/May 1994	*Charles Darwin*	Goban Spur
May 1994	*Belgica*	Goban Spur, La Chapelle Bank
June 1994	*Charles Darwin*	Goban Spur
September 1994	*Meteor*	Goban Spur
March 1995	*Belgica*	Goban Spur, La Chapelle Bank
June 1995	*Charles Darwin*	Goban Spur
August/September 1995	*Discovery*	Goban Spur
September 1995	*Belgica*	Goban Spur, La Chapelle Bank
October 1995	*Discovery*	Goban Spur

thermocline. The surface mixed-layer depth was determined for every CTD cast. At many stations, a well-defined thermocline was present, and it was straightforward to determine mixed-layer depths. But at some stations, the vertical structure was complex and variable, as a result of internal tides, near-surface diurnal heating/cooling, and other factors. In some cases, there was no unique mixed layer but a sequence of layers had developed. Where other CTD profiles were available within a period of 2 d, these repeat profiles were used to provide an indication of variability in the mixed-layer depth estimates (Huthnance et al., 2001).

2.3. Nutrient concentrations

On all cruises, the analysis of nutrients was carried out immediately after sampling. During the *Belgica* cruises, ammonium was determined according to the manual method of Koroleff (1969) with a detection limit of $0.05\,\mu mol\,l^{-1}$. Nitrate and nitrite were measured using a Technicon AutoAnalyser II with a detection limit of $0.05\,\mu mol\,l^{-1}$. Phosphate also was determined manually on board following the method of Grasshoff et al. (1983) with a detection limit of $0.01\,\mu mol\,l^{-1}$ using a 10-cm cell. Silicate was either measured manually on board using the procedures described in Grasshoff et al. (1983) or in the laboratory using an SKALAR AutoAnalyser following the method provided by the manufacturer. The detection limits of silicate are 0.02 and $0.05\,\mu mol\,l^{-1}$ for manual determination using a 5-cm cell and for automated method, respectively. On the *Darwin* cruises, ammonium, nitrate plus nitrite, and silicate were analysed by the methods of Hydes (1984) and nitrate by the method of Grasshoff et al. (1983).

2.4. Phytoplankton biomass

Phytoplankton biomass was estimated from pigment analysis by HPLC (Barlow et al., 1993, 1995), by fluorometric analysis (Holm-Hansen et al., 1965), and by spectrophotometric analysis

(Parsons et al., 1984). HPLC also gives information on the taxonomic composition of the phytoplankton assemblages. Phytoplankton identification also was determined on a small number of cruises by microscope analysis of the phytoplankton species present in water samples preserved with Lugol's iodine (Rees et al., 1999). The most comprehensive data to describe the decadal mean seasonal changes in phytoplankton biomass were provided by the Continuous Plankton Recorder (CPR) survey index of green colour. The colour of the silk in the CPR survey (Colebrook, 1960) has been shown to provide a useful index of phytoplankton biomass present in the surface 10 m. Data obtained for each of the OMEX regions for the period 1963–1995 have been used to calculate a climatological mean for each calendar month.

2.5. Phytoplankton production

Primary production was measured by the incorporation of ^{14}C-bicarbonate as described by Rees et al. (1999). Experiments were carried out in polycarbonate bottles, following JGOFS protocols (IOC, 1994) to reduce trace metal contamination. Water samples were taken from 8 to 10 depths before dawn and incubated for 24 h either in situ at the depth from which the water sample was taken, or in an on-deck incubator with filters to simulate the light quantity and colour at the appropriate depths. Each bottle was inoculated with 370 kBq (10 μCi) $NaH^{14}CO_3$ and transferred to the incubation system before dawn and incubated until dusk. In situ samples were brought on board at dusk and maintained at surface sea-water temperature in the dark overnight. On-deck incubations had their graded light screens replaced with dark screens to ensure that they were not affected by the ship's lights. Incubations were terminated after 24 h by filtering each sample sequentially through 5, 2-, and 0.2-μm pore size polycarbonate filters; the filters were dried and either counted on board ship or stored in a desiccator until return to the laboratory. ^{14}C was measured in a liquid scintillation counter, the efficiency of which was determined with an external standard, channels ratio method.

Due to the limited ship time available, an alternative method was used to evaluate the primary production at La Chapelle Bank. Water samples collected just before dawn were incubated for 6 h under variable light intensities from an artificial constant-light source, with spectral characteristics as similar as practicable to sunlight. This method allows a relationship to be established between the carbon fixation rate and the light intensity, which is characteristic of the phytoplankton assemblage present and its physiological state. The relation suggested by Platt et al. (1980) was used, enabling the characterisation for each experiment of the maximum photosynthetic capacity, the photosynthetic efficiency and the index of photoinhibition of the phytoplankton present at the depth of the oxygen maximum. The maximum photosynthetic capacity and chlorophyll content were also measured at other depths between 0 and 100 m by incubating water samples under saturated light condition. The vertical attenuation of light was determined using a quantameter and the daily incident light intensity recorded at a high, unshaded position on the ship.

To obtain the integrated daily production, a mean value for the irradiance during daylight hours at the air–sea interface multiplied by the day-length was used (see Kirk (1994) for discussion). The validity of this approach was tested at three stations by comparing the values obtained with those of in situ production measurements described as above. There is an agreement between the two methods within an error of $\pm 15\%$.

2.6. New production estimates

Assimilation rates for NO_3 (ρNO_3) and NH_4 (ρNH_4) were determined using the stable isotope ^{15}N. Replicate samples from each depth were incubated in clear polycarbonate bottles with $^{15}N\text{-}NO_3^-$ and $^{15}N\text{-}NH_4^+$ added at concentrations of between 0.03 and 0.1 μmol l^{-1}. Samples were incubated for 24 h and filtered onto ashed Whatman GF/F filters, which were then washed with filtered sea water and stored frozen until return to the laboratory. The filters were oven-dried at 50°C for 12 h before analysis and atom% ^{15}N was measured either by continuous flow nitrogen analysis-mass spectrometry (Europa Scientific Ltd., UK) using the techniques described in Barrie et al. (1989) and Owens and Rees (1989) or by emission spectrometry (Jasco NIA-1 and N-151 ^{15}N analysers) using the techniques described in Fiedler and Proksch (1975). Full details of the methods used are set out in publications by Elskens et al. (1997) and Rees et al. (1999). Rates of assimilation were calculated from the equations of Dugdale and Goering (1967).

2.7. Remote sensing images

Satellite estimates of sea-surface temperature (SST) were obtained from the NASA advanced very high resolution radiometer (AVHRR) pathfinder data set (Vazquez et al., 1994), which provides global SST for 1987–1993. The Pathfinder-SST are an improvement upon earlier data sets through development of enhanced SST-retrieval algorithms and cloud-masking routines. The SST data are available as monthly fields on an equal angle grid, giving a resolution of 9 km at the equator. The data were spatially averaged within the boxes shown in Fig. 1, and data for each month were averaged to give climatological means for 1987–1993.

Similar monthly climatological averages of phytoplankton pigment are available on an 18-km (at the equator) equal angle grid from the NASA coastal zone color scanner (CZCS: Feldman et al., 1989). The CZCS operated from 1978 to 1986, although data coverage in later years was poor, and so the averages are skewed to the early years of operation. The CZCS data were averaged to produce means within the OMEX boxes. Since the atmospheric correction is valid for solar zenith angles $<65°$ (Gordon et al., 1988), only data for April through September were used. In addition to the problem of high winter solar zenith angle, images of the OMEX shelf area in winter and early spring exhibit enhanced reflectance due to suspended particles, and this contributes to erroneous estimates of pigment concentration (Joint and Groom, 2000).

2.8. Bacterial activity

Bacterial production was determined from rates of incorporation of [methyl-^{3}H] thymidine and of L-[4,5-^{3}H] leucine (Amersham International plc, UK). Stock ^3H solutions were prepared using sterile glassware and stored in pharmaceutical-grade serum bottles that had been pre-treated according to JGOFS protocols (IOC, 1994). Stock ^3H solutions were prepared in sterile, 0.2-μm filtered, Milli-Q water and stored at 2°C. A fresh stock bottle was used for each experiment. ^3H-thymidine incorporation experiments followed the methods of Fuhrman and Azam (1982) and ^3H-leucine incorporation experiments those of Simon and Azam (1989) modified to include the cold trichloroacetic acid (TCA) extraction method of Chin-Leo and Kirchman (1988). The samples were routinely incubated for 1 h, but time-course assays showed that incorporation was

linear for 2 h and frequently longer. Samples were counted in an LKB, Rackbeta 1219, liquid scintillation counter; counting efficiency was determined by an external standard, channels ratio method and checked by the occasional addition of internal standards.

2.9. Microzooplankton herbivory and respiration

Microzooplankton identification and biomass estimation was by microscope analysis of water samples preserved with Lugol's iodine or glutaraldehyde. Microzooplankton grazing on phytoplankton was determined by a modification of the dilution/grazing technique of Landry and Hassett (1982) and measured changes in chlorophyll content. Hence the microzooplankton grazing rates are confined to estimates of herbivory and do not include grazing of microzooplankton on bacteria. Changes in chlorophyll concentration were converted to carbon units by applying a constant carbon : chlorophyll ratio of 59 throughout the year. Microzooplankton respiration was estimated from biomass using the method of Caron et al. (1990). Respiration was estimated for each size category of microzooplankton assuming a Q_{10} of 2 and an RQ of 1.

2.10. Mesozooplankton biomass and herbivory estimates

Mesozooplankton biomass was determined from the CPR data as described by Batten et al. (1999). The abundance recorded in each CPR sample was multiplied by a taxon-specific biomass and converted to carbon using published carbon values for zooplankton taxa (Schneider, 1989); the summed values for the individual taxa then give an estimate of total mesozooplankton biomass. These data on biomass were then used to estimate mesozooplankton respiration and ingestion rates, by applying an allometric model (Ikeda and Motoda, 1978); respiration was estimated as a function of individual body weight and temperature. It was assumed that respiration is a constant fraction of ingestion. Respiration of each species or size group was calculated from the allometric relationship

$$R = aW^{b}$$

using the temperature relationship of Ikeda and Motoda (1978). Constant a has the value of $10^{(0.0254\,T-0.126)}$ and constant b the value of $-0.011T + 0.892$ (Ikeda and Motoda, 1978). An RQ of 0.8 was assumed to convert oxygen consumed to carbon, hence giving estimates of daily respiration rate for each species. These values were then applied to all the individuals of one species present in a sample, and the estimates for each species present were summed to give total mesozooplankton respiration. Ingestion rate for each species was calculated from the respiration estimates by assuming an assimilation efficiency of 0.7 and a gross growth efficiency of 0.3. Total grazing was calculated by summing the grazing estimates for all species and size groups within a sample.

The temperature for the different OMEX regions at the time of the CPR surveys was determined from sea-surface temperatures obtained from satellite AVHRR data. Hence seasonal, temperature-compensated, carbon-specific grazing rates could be estimated for each of the OMEX regions.

3. Results

3.1. Surface mixed-layer depth

The water column in the region is well mixed in winter and strongly stratified in summer. Fig. 2 shows an annual synopsis of the mixed-layer depth, which is derived by taking mean values for each month from all of the data available between 1993 and 1995; therefore Fig. 2 is an idealised representation of mixed-layer depth and does not show interannual variability. Nevertheless, it does show differences in timing of stratification across the five regions and changes in mixed-layer depth. The onset of stratification in the spring occurs at different times and tends to be earliest on the shelf in April and latest at the stations in deepest water. However, there is great variability due to internal tides. Often there is no unique mixed layer but a sequence of layers with several thermoclines. The timing of sampling also can give a false impression of stratification. The April values for the OMEX 1 region in Fig. 2 were obtained in spring 1994 at a time of variable weather with transient stratification breaking down during storms. The sequence is described in detail by Rees et al. (1999). Hence, the level of detail in Fig. 2 is insufficient to describe the events that occur in the spring, with water column stabilisation occurring over a few days and the exact timing varying from year to year. However, the data do highlight the differences in mixed-layer depth in the summer months, with the shallowest surface mixed-layer (at about 30 m) on the shelf and at La Chapelle Bank in July and a gradual deepening of the mixed-layer in September and October. The most variability in mixed-layer depths occurs in the OMEX 1 region, where satellite thermal images suggest that upwelling takes place.

3.2. Nutrient concentrations

One of the achievements of the OMEX Project is that data were collected in all four seasons (Hydes et al., 2001). The recent EU-MAST-NOWESP Project compiled all available

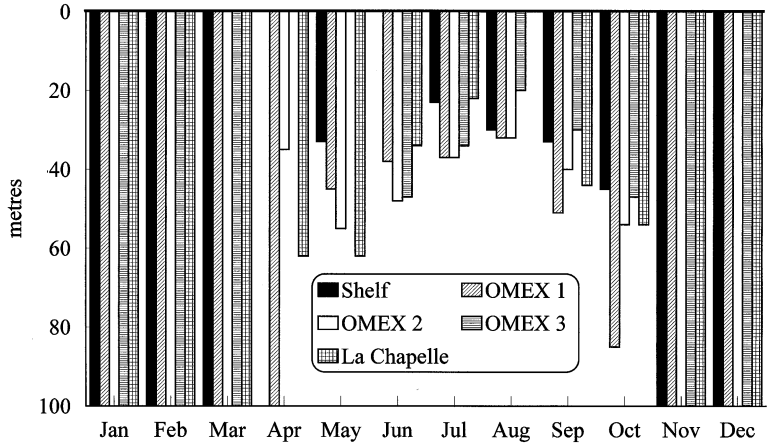

Fig. 2. The depth of the surface mixed layer for each region throughout the year. In the winter months, > 100 m indicates a well-mixed water column.

hydrographic and nutrient data for North West European Shelf Seas; even in such a well-studied area, there are gaps in the data sets, particularly for the winter months. Knowledge of winter concentrations is important, as the extent of deep winter mixing determines the concentrations of nutrients in the surface waters at the onset of seasonal stratification and the extent of the phytoplankton spring bloom. Winter data are available from two cruises in January 1994 (Table 1). Sampling by the *Meteor* was restricted by weather conditions to five stations, from ca. 11°W to 14°W at 49°N. The water column was well mixed to a depth of 300 m, and nutrient concentrations were homogeneous; the concentration of nitrate was 7.7 $\mu mol\,l^{-1}$, silicate was 2.8 $\mu mol\,l^{-1}$, and phosphate was 0.50 $\mu mol\,l^{-1}$.

The *Charles Darwin* cruise was able to sample a larger region, from La Chapelle Bank, north to the Goban Spur and into the Celtic Sea, but because of equipment malfunction, only nitrate concentrations were measured. Over the whole region sampled, nitrate concentrations ranged from 6.5 to 10.4 $\mu mol\,l^{-1}$ in a salinity range of 35.62–34.78. At the shelf break, the water column was less well mixed than at the stations sampled by the *Meteor* and nitrate concentration was correlated to water temperature; nitrate concentration ranged from 7 $\mu mol\,l^{-1}$ at 11.6°C to 8.7 $\mu mol\,l^{-1}$ at 11.0°C.

In summer, nitrate concentrations were depleted below the limit of detection of the auto-analyser methods. For example, in August 1995 nitrate concentrations were less than 0.01–0.05 $\mu mol\,l^{-1}$ in the surface mixed layer. On this cruise, 31 samples were taken from water above the thermocline and nitrate was undetectable in all samples; the average phosphate concentration was 0.02 $\mu mol\,l^{-1}$ (range 0.00–0.07 $\mu mol\,l^{-1}$) and the average silicate concentration was 0.4 $\mu mol\,l^{-1}$ (range 0.2–0.6 $\mu mol\,l^{-1}$).

3.3. Phytoplankton biomass

Fig. 3 shows the CPR Greenness Index for each region, with each month represented by the mean value of every sample obtained between 1963 and 1995. These data, therefore, have the

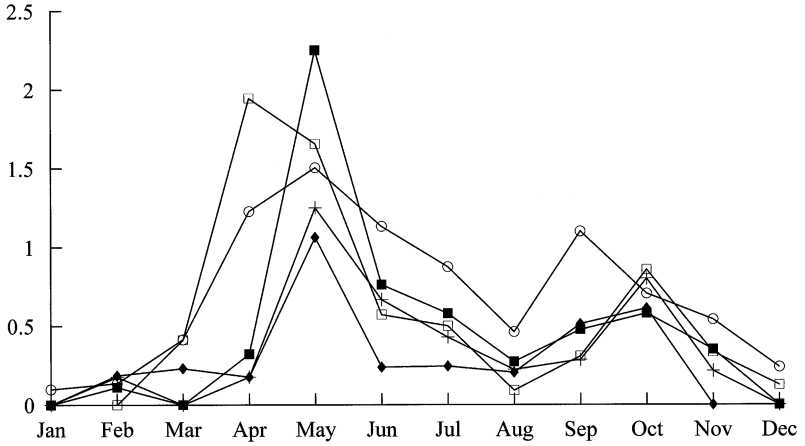

Fig. 3. The CPR colour index (in arbitrary units) as an indicator of phytoplankton biomass for every month at each region. The data are climatological mean values determined for the period between 1963 and 1995. The regions are the Celtic Sea Shelf (□), the OMEX 1 region (■), OMEX 2 (+), OMEX 3 (♦), and La Chapelle Bank (○).

greatest sampling density and frequency for phytoplankton biomass in the Celtic Sea, and provide the best description of the mean-decadal seasonal cycle of abundance. The shelf region shows the earliest increase in phytoplankton biomass in the spring, with a bloom that lasts for over 2 months in April and May. The spring bloom is of much shorter duration at the shelf edge and oceanic stations (OMEX 1–3). At all regions of the Goban Spur, phytoplankton biomass declines from June to a minimum in August. There is an autumn bloom, which is most pronounced at the shelf stations and at OMEX 2. The seasonal abundance of phytoplankton is very different at La Chapelle Bank, with a broad peak of abundance that increases in April and extends throughout the summer months with a slow decline in abundance from May. There is a very pronounced autumn peak that declines much more slowly than at the Goban Spur through November and December.

The CPR data give a good indication of seasonal changes in total phytoplankton biomass, but the CPR silk has too coarse a mesh to be useful as a quantitative sampler of small phytoplankton cells or to determine phytoplankton species succession. However, during the OMEX project, phytoplankton pigments were analysed by HPLC and are useful as indicators of the major phytoplankton taxa. Table 2 lists the concentrations of major pigment classes; the data are based on samples taken throughout the water column, and the concentrations are expressed as mg m^{-2}; that is, integrated to the base of the surface mixed layer, or to 100 m if the water column was well mixed.

Apart from the spring bloom, depth-integrated chlorophyll *a* concentrations actually show little variation with season. For example, at OMEX 2, the maximum chlorophyll *a* concentration measured in the surface mixed layer in April was 22.7 mg m^{-2}, but the total quantity of chlorophyll *a* in the upper 100 m in January was 14.5 mg m^{-2}. Of course, the surface mixed-layer depth varied and the depth-integration was done to 35 m in April and to 100 m in January. So in January, much of the pigment is present below the depth of light penetration. Sampling may not always have coincided with the maximum biomass; the highest concentration measured was at OMEX 1 in April 1995, when a concentration of 95.2 mg m^{-2} was measured.

There were significant changes in the phytoplankton taxa present. Photosynthetic pigments have been used as biomarkers to indicate the most abundant phytoplankton taxa (Table 2). Winter samples are characterised by the presence of 19′-hexanolyoxyfucoxanthin, an indicator of prymnesiophytes, 19′-butanoyloxyfucoxanthin, indicating the presence of pelagophytes and small concentrations of fucoxanthin, a marker for diatoms, and zeaxanthin, indicating the presence of cyanobacteria. The spring phytoplankton assemblages were dominated by prymnesiophytes, diatoms, pelagophytes, prasinophytes (from the presence of chlorophyll *b*), and dinoflagellates (indicated by elevated peridinin concentrations). In the summer months, the most abundant pigment was 19′-hexanoyloxyfucoxanthin, indicating the dominance of prymnesiophytes. Autumn assemblages were again a mixture of prymnesiophytes, diatoms, pelagophytes, dinoflagellates, and cyanobacteria. Prymnesiophytes were an important component of the phytoplankton assemblage in all seasons.

A small number of water samples also were analysed for phytoplankton species abundance, and cells $> 5\,\mu m$ were identified and counted. In April/May 1994, the spring bloom was dominated by the diatoms *Nitzschia delicatissima* (3×10^5 cells l^{-1}), *Nitzschia seriata* (3.5×10^5 cells l^{-1}), *Thalassionema nitzschiodes* (1.8×10^5 cells l^{-1}) and *Chaetoceros* spp. (1.4×10^5 cells l^{-1}), with the presence of *Phaeocystis* spp. at some stations. A number of dinoflagellate species (e.g., *Ceratium*

Table 2
Photosynthetic pigment concentrations, expressed as depth-integrated values (mg m^{-2}) to the base of the surface mixed layer, or to 100 m if the water column was well mixed

Date	chla[a]	chlb[b]	per[c]	but[d]	fuco[e]	hex[f]	zea[g]
OMEX 1							
July 93	16.23	1.83	0.43	4.17	1.75	10.33	0.41
April 94	95.17	6.29	5.07	13.47	26.66	31.46	0.79
July 95	3.11	0.21	0.40	0.53	0.23	1.50	0.14
October 95	27.52	2.41	2.00	4.82	2.52	13.68	1.45
OMEX 2							
July 93	16.10	2.75	0.48	3.63	1.87	10.75	0.43
September 93	11.90	1.47	0.44	2.23	0.76	5.94	1.01
January 94	14.53	2.23	0.14	3.82	1.82	6.48	0.25
April 94	22.67	2.59	0.79	3.96	4.16	8.99	0.35
June 95	19.94	0.98	0.37	2.64	4.04	14.59	0.53
July 95	11.69	0.51	1.63	2.15	0.87	5.71	0.22
September 95	13.08	1.40	1.68	1.50	1.15	6.45	0.87
October 95	25.33	2.21	0.55	6.92	2.20	14.97	1.26
OMEX 3							
July 93	9.22	0.83	0.30	1.91	1.30	5.42	0.41
September 93	10.83	1.93	0.79	2.42	1.06	5.75	0.62
January 94	13.73	2.12	0.16	3.70	1.73	6.06	0.34
April 94	6.14	0.98	0.34	0.89	1.19	2.65	0.14
June 95	12.84	0.44	1.22	1.48	1.62	9.53	0.22
July 95	27.02	1.38	5.85	3.42	2.80	10.63	0.20
September 95	3.89	0.21	0.42	0.34	0.33	1.68	0.50
October 95	24.95	2.29	1.07	6.32	1.81	14.16	1.49
La Chapelle	Bank						
September 93	10.37	0.48	0.82	2.21	3.98	1.26	0.07
January 94	17.41	2.99	0.21	4.18	2.45	7.32	0.35
June 95	11.68	1.62	0.15	0.67	1.62	3.48	0.03
September 95	31.84	7.99	1.05	5.45	5.46	14.32	0.94

[a] Chlorophyll *a* (total phytoplankton biomass).
[b] Chlorophyll *b* (chlorophytes).
[c] Peridinin (dinoflagellates).
[d] 19′-butanoyloxyfucoxanthin (pelagophytes).
[e] Fucoxanthin (diatoms).
[f] 19'-hexanoyloxyfucoxanthin (prymnesiophytes).
[g] Zeaxanthin (cyanobacteria).

lineatum, *Heterocapsa minima*, and *Prorocentrum compressum*) were present at cell densities of ca. 100 cells l^{-1}. In July 1993, most of the phytoplankton biomass was small unidentified flagellates. Of the > 5-μm phytoplankton, a diverse assemblage of dinoflagellates was present at cell densities of ca. 100–200 cells l^{-1}; the species included *Ceratium furca*, *C. fusus*, *C. lineatum*, *Gonyaulax*

polygramma, and *Prorocentrum dentatum*. In October 1995, there were large numbers of diatoms, including *Chaetoceros* spp. (1×10^5 cells l^{-1}), *Nitzschia delicatissima* (2×10^5 cells l^{-1}) and *N. seriata* (2×10^5 cells l^{-1}); again, there was also a diverse assemblage of dinoflagellates and large numbers of small (ca. 2 μm) unidentified flagellates.

3.4. Phytoplankton production

Primary production was measured on a number of cruises in the OMEX project by either in situ or on-deck incubations. Since the size of phytoplankton has strong consequences for the fate of that production, estimates were made for three size fractions of phytoplankton cells, >5, 5–2, and <2 μm. However, the seasonal coverage was small, with most measurements being made in the spring and summer months. The relatively small number of determinations also presents difficulties in estimating production for the different OMEX regions, and estimates of annual primary production are constrained by the relative lack of measurements during the OMEX project—due to some extent, to the difficult weather conditions in that area. Therefore, the data have been supplemented with unpublished data for Little Sole Bank, an adjacent region of the Celtic Sea shelf break, which was sampled in spring 1990 and 1991 (I. Joint, unpublished data). By incorporating data from the Celtic Sea shelf (Joint et al., 1986), an estimate of daily primary production has been made for each month (Fig. 4). Measurements in the Goban Spur area in the OMEX project were made in April and the first week of May 1994, July 1993, and October 1995, the Little Sole Bank data are for mid-June 1991 and mid-May 1992, and all other estimates are taken from Joint et al. (1986).

Primary production in the winter was dominated by small phytoplankton cells; from November to March, cells <5 μm were responsible for 70–86% of the primary production, which was not insignificant at ca. 200 mg C m^{-2} d^{-1}. The spring bloom was dominated by larger (>5 μm) phytoplankton cells, and total primary production increased to >1 gC m^{-2} d^{-1}. The exact timing of the spring bloom is difficult to determine since the data shown in Fig. 4 for April and May were collected in different years. The CPR colour index (Fig. 3) suggests that the spring bloom on the shelf lasts for about 2 months, but may be shorter at the shelf break and deep ocean sites and longer at La Chapelle Bank. Therefore, the extended production throughout April and May in Fig. 4 is probably more representative of the shelf than other regions. There may be an overestimation of the spring bloom production in this aggregate of data from different years. The production of the >5-μm fraction declined steadily after the spring bloom and by July, large cells were responsible for less than 50% of the total phytoplankton production. In the autumn, picoplankton (<2 μm) were the most productive fraction. The data in Fig. 4 for October were obtained in 1995, when there was no evidence for an autumn increase in biomass or production. However, the CPR colour index routinely shows an increase in phytoplankton biomass. Therefore, 1995 appears to be an anomalous year and there may usually be an increase in production in October, which is not reflected in Fig. 4.

The lack of seasonal coverage of primary production measurement at La Chapelle Bank during the OMEX project was also partially compensated by using unpublished data for the region, obtained between 1989 and 1993, in the framework of a national Belgian programme (R. Wollast et al., unpublished data). A total of 17 data sets were finally available for the area of La Chapelle Bank. Nevertheless, the winter period, November–February, was never covered and here also

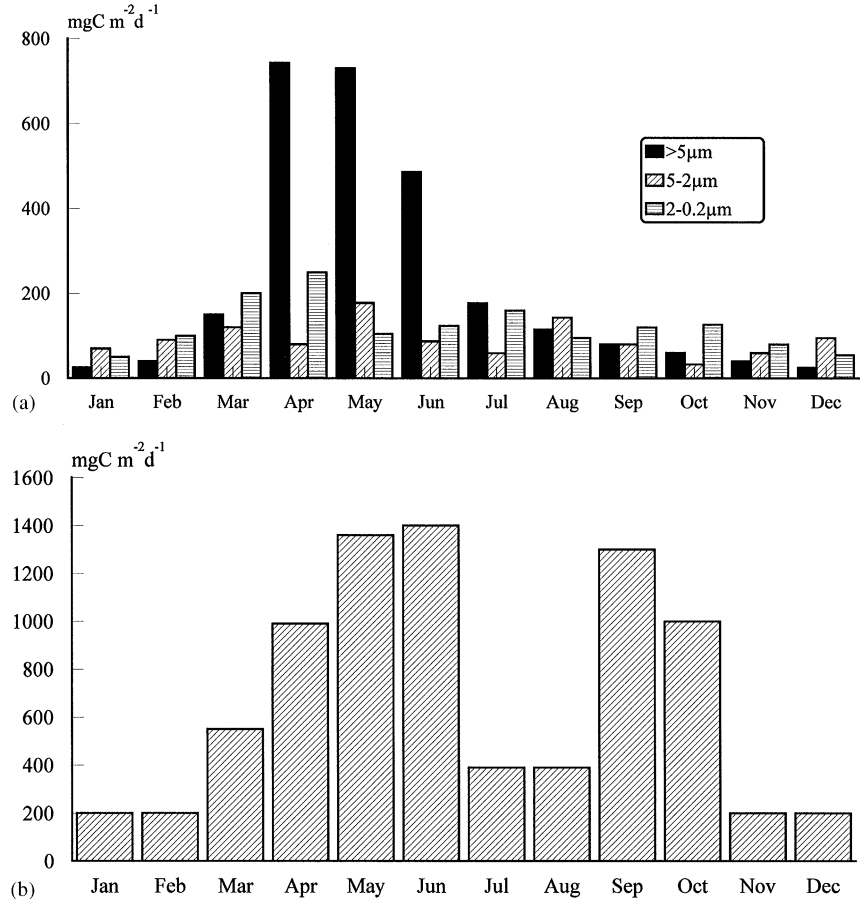

Fig. 4. Estimated daily primary production (mg C m^{-2} d^{-1}) in each month for three size fractions of phytoplankton at (a) Goban Spur and (b) total phytoplankton production at La Chapelle Bank.

data from the Celtic sea shelf (Joint et al., 1986) were incorporated for these months. No primary production measurements were performed during August but, by analogy to Goban Spur, it is assumed that it is low and similar to the production in July. The mean monthly productions at La Chapelle Bank (Fig. 4b) show the existence of a large spring bloom extending from March to June and a second bloom in September and October. This observation is in good agreement with the data from the CPR shown in Fig. 3.

A few size-fractionated carbon uptake measurements were carried out at La Chapelle Bank and indicate that >2-μm phytoplankton cells represent from 29% to 65% of the total production. Unlike the situation at the Goban Spur, the dominance of >2-μm phytoplankton was observed only in mid-September 1995 when the autumn bloom seemed to have occurred. In late April 1994, at La Chapelle Bank the production was slightly dominated (59%) by the small size class (0.2–2 μm), while >2-μm cells accounted for 80% of the total production along the Biscay margin, 60–120 nautical miles southeast of the area. It is interesting that a week later, in contrast

to La Chapelle Bank, the Goban Spur was dominated by the fraction larger $>2\,\mu m$, as often observed during a spring bloom. The paucity of data on size-fractionated production in the region of La Chapelle Bank does not allow a clear seasonal trend to be established.

The annual primary production at La Chapelle Bank (Fig. 4b) probably approaches $245\,g\,C\,m^{-2}\,a^{-1}$, assuming a carbon fixation rate of $200\,mg\,C\,m^{-2}\,d^{-1}$ for the winter period and if the August rate was similar to that observed in July. The annual production is estimated to be significantly higher than for the Goban Spur, but is consistent with the higher chlorophyll concentrations observed by both the remote sensing observations and the CPR results (Fig. 3). The higher production may be explained by the steeper slope at La Chapelle Bank compared to the Goban Spur, which induces greater vertical mixing and nutrient supply.

3.5. New production estimates

The uptake of ammonium and nitrate has been measured using ^{15}N as a tracer. Although a large number of measurements were made, the seasonal coverage is not complete. In contrast to primary production, there are no other studies in the Celtic Sea to supplement the data obtained in OMEX. Therefore, obtaining a seasonal estimate of new production involves considerable interpolation. Table 3 shows values for the *f*-ratio, estimated by the Plymouth Marine Laboratory (PML) and Vrije Universiteit Brussel (VUB) groups. When measurements were made in the same month by the two groups, albeit on different cruises, there was generally good agreement. However, in July 1993, the PML group obtained higher values for the *f*-ratio than that measured by VUB, and in September the VUB estimate was greater than the PML. The differences are largely the result of the different regions sampled, because only the VUB group sampled at La Chapelle Bank.

Table 3
Estimated *f*-ratio for each month determined by the PML and VUB groups with monthly primary and new production ($g\,C\,m^{-2}\,month^{-1}$). Values in parentheses are estimated or extrapolated values

Month	Year of PML data	*f*-ratio (PML)	Year of ULB data	*f*-ratio (VUB)	Carbon fixation	New production
January		(0.5)			4.5	2.3
February		(0.5)			6.4	3.2
March			1995	0.7	18.3	12.8
April	1994	0.8	1994	0.74	32.2	22.5
May	1994	0.6			31.4	18.6
June			1992	0.33	20.9	6.9
July	1993	0.25		0.14	12.3	3.1
August		(0.3)			11	3.3
September	1995	0.25	1995	0.39	8.4	2.1
October	1995	0.35	1995	0.31	6.8	2.4
November		(0.4)			5.4	2.2
December		(0.45)			5.4	2.4
Annual ($g\,C\,m^{-2}\,a^{-1}$)					162	81.8

Table 3 shows the extrapolations that have been made to evaluate seasonal new production; data in parentheses are estimated values. The largest gap in the data is for the winter months. The VUB group measured *f*-ratios of 0.47–0.81 in March 1995, with a mean value of 0.64; The variability appeared to correlate with solar irradiation, nitrate uptake rate apparently being more dependent on light than ammonium uptake. The PML group measured nitrate and ammonium uptake in April 1994 at a number of stations before stratification occurred (Rees et al., 1999). In well-mixed waters, the *f*-ratio was close to 0.5, with comparable rates of ammonium and nitrate assimilation, even when nitrate concentrations were at their winter maximum. Therefore, as a consequence of the reduced light and day length in the winter months, the *f*-ratio is assumed to increase slowly from the low values in the autumn months and to be about 0.5 in January and February. Measurements in the winter months are clearly needed to confirm this assumption. The *f*-ratio increases to between 0.7 and 0.8 during the spring bloom and declines to low values in the early summer and through the autumn.

The *f*-ratios have been combined with the primary production measurements (Fig. 4) to give an estimate of monthly new production, i.e., production that results from the utilisation of nitrate by the phytoplankton assemblage. The data in the final column of Table 3 were obtained by multiplying the total primary production for each month by the *f*-ratio, measured by either the PML or VUB groups, or estimated by extrapolation. New production in the spring bloom is ca. $20\,g\,C\,m^{-2}\,month^{-1}$ and declines to ca. $2\,g\,C\,m^{-2}\,month^{-1}$ for the rest of the year, including the winter months. The annual new production estimate is $81.8\,g\,C\,m^{-2}$, that is ca. half of the total phytoplankton production. It is worth emphasising that this estimate is applied to the region as a whole and does not attempt to account for any enhanced production due to upwelling at the shelf break.

3.6. Remote sensing images and estimation of new production

Given the difficulties in obtaining sufficient field data to make an estimation of seasonal production and given that the best evidence for upwelling events at the shelf break originates from satellite images, we have applied the technique of Sathyendranath et al. (1991), using remote sensing as a tool to study the dynamics of this region. Nitrate concentration was strongly correlated with sea-surface temperature in June 1995 ($r^2 = 0.927$), and the algorithm has been used to estimate nitrate concentration from SST values derived from the AVHRR in the surface waters of the OMEX region. This approach provides synoptic estimates of nitrate distribution. Fig. 5 shows that, as Sathyendranath et al. (1991) found for Georges Bank, there is also a good relationship between nitrate concentration and *f*-ratio, when data for *f*-ratio obtained by both the PML and the VUB are plotted against nitrate concentration. These *f*-ratios were obtained for water samples taken from the upper 15 m and do not include any measurements made at the base of the mixed layer or within the thermocline. The equation of the fitted line is

$$f\text{-ratio} = 0.118 \log_e (\text{nitrate concentration}) + 0.559$$

with r^2 of 0.73. Examination of the residuals in this curvilinear regression shows that the additive error ε (Elskens et al., 1999) is normally distributed and that *f*-ratio estimates are provided with relative uncertainties of 57%, 42%, and 20% for nitrate concentrations <0.1, 0.1–1, and $>1\,\mu mol\,l^{-1}$, respectively. The significance validity limits of the predicted *f*-ratio values and

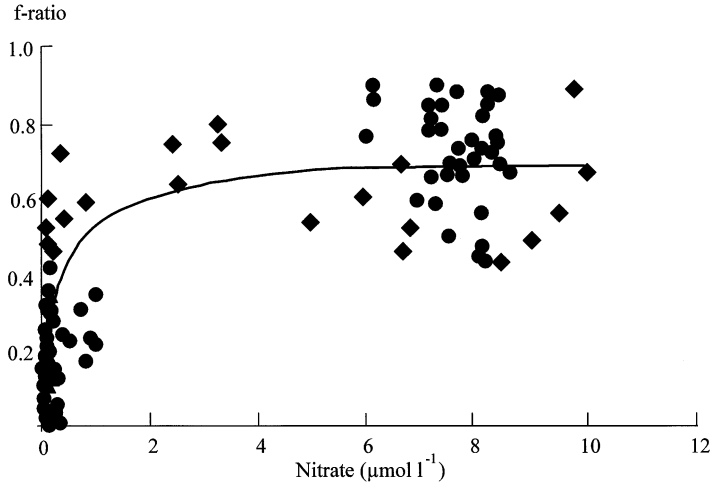

Fig. 5. Relationship between *f*-ratio, as determined experimentally by the incorporation of ^{15}N nitrate and ammonium, and nitrate concentration in the surface 15 m. Determinations made by the PML (●) and by VUB (♦).

statistical properties in non-linear regression models of *f*-ratio vs. nitrate concentration are discussed by Elskens et al. (1999). With these uncertainties in mind, the equation above was used to obtain an average estimate of new production for the Goban Spur (Fig. 6).

Observations obtained in the OMEX Project also have been used to develop a simple empirical algorithm between primary production and pigment concentration. This has been used with the CZCS phytoplankton pigment climatological data to estimate monthly mean production for the period 1978–1986, albeit skew to the early years of the operation of the sensor. Limitations in the atmospheric correction limit the analysis of CZCS data to April through September. Table 4 gives a comparison of monthly primary production, estimated from CZCS ocean colour, with the measurements made in the OMEX project. Comparisons also are shown of *f*-ratio and new production, determined by the method of Sathyendrenath et al. (1991), with estimates from direct experimentation. There is general agreement with the satellite estimate of primary production of $90\,g\,C\,m^{-2}$ per half year (April through September), contrasting with $116\,g\,C\,m^{-2}$ per half year from Fig. 4. Similarly, the satellite-based estimate of new production is $46\,g\,C\,m^{-2}$ per half year, which compares with $57\,g\,C\,m^{-2}$ per half year estimated for the same period from the data in Table 3. Therefore, the estimates based on satellite data are consistent with direct estimates from field data.

3.7. Microzooplankton herbivory

The abundance and herbivory rate of microzooplankton have been determined by Edwards et al. (2001) for the Goban Spur sites; microzooplankton were not sampled at La Chapelle Bank, and only one estimate is available for the shelf region. Fig. 7 shows the seasonal changes in daily grazing rate, which are integrated to the depth of the surface mixed layer. As such, they are directly comparable with primary production rates and have the same units of $mg\,C\,m^{-2}\,d^{-1}$. Grazing rates were low in the winter and were between 29 and $43\,mg\,C\,m^{-2}\,d^{-1}$ in January.

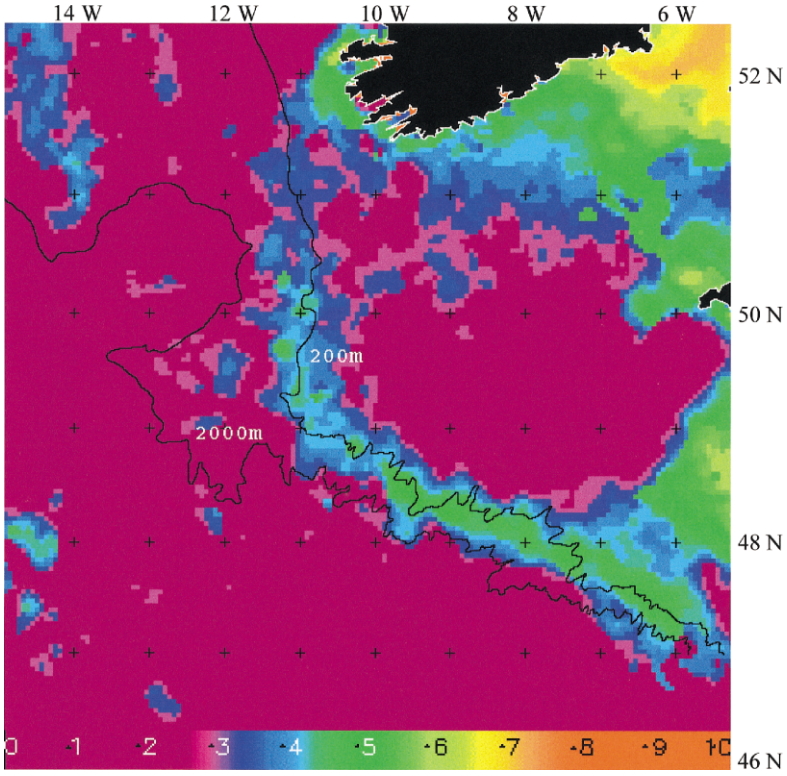

Fig. 6. *f*-ratio for the Celtic Sea region calculated from the relationship between sea-surface temperature (from AVHRR) and nitrate concentration and applying the nitrate : *f*-ratio relationship (Fig. 5) determined for the Celtic Sea.

Table 4
Comparison of primary and new production estimated from satellite data with experimental determinations

Date	C fixation (measured)	C fixation (satellite)	*f*-ratio (measured)	*f*-ratio (satellite)	New production (measured)	New production (satellite)
April	32.2	15.7	0.8	0.8	22.5	13
May	31.4	23.1	0.6	0.7	18.6	16.7
June	20.9	15.9	0.25	0.2	6.9	3.3
July	12.3	10.5	0.25	0.2	3.1	2.2
August	11	11.5	0.3	0.2	3.3	2.4
September	8.4	14.1	0.25	0.6	2.1	8.6
Annual ($g C m^{-2} a^{-1}$)	116	91			57	46

Although grazing was higher in April and May, at the time of the phytoplankton spring bloom, the highest values of microzooplankton grazing were measured at OMEX 1 in June when the rate was $673 mg C m^{-2} d^{-1}$. However, there was considerable variability in grazing rate between the different regions and at OMEX 3 in June, the microzooplankton grazing rate was only $102 mg C m^{-2} d^{-1}$; grazing at OMEX 3 was also low in April and July. Grazing was low in all

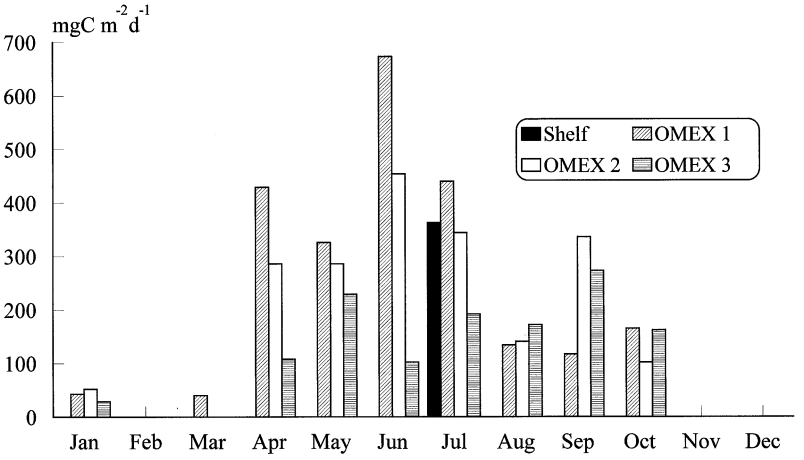

Fig. 7. Depth-integrated microzooplankton grazing ($mg\,C\,m^{-2}\,d^{-1}$) for four regions at the Goban Spur.

regions in August at ca. 130–170 $mg\,C\,m^{-2}\,d^{-1}$ and increased slightly in September to 237 and 336 $mg\,C\,m^{-2}\,d^{-1}$ at OMEX 2 and 3.

3.8. Mesozooplankton biomass and herbivory

The CPR survey provides an excellent database to construct a climatological mean of mesozooplankton biomass, since data are available for every month of the year from 1963 to 1995. Fig. 8 shows the biomass of mesozooplankton at 10 m in each of the regions studied at the Celtic Sea shelf break. The highest biomass was recorded on the shelf in May. The biomass increased in April from winter minima in all regions, but there was significantly more mesozooplankton on the shelf than in other regions; in May the biomass on the shelf was 12 $mg\,C\,m^{-3}$, at La Chapelle Bank it was 7 $mg\,C\,m^{-3}$, and at OMEX 3 it was 3.3 $mg\,C\,m^{-3}$. There was an autumn increase in biomass in October at OMEX 1 and 2, but none was apparent at the shelf region, OMEX 3 nor La Chapelle Bank; there was a slight increase in August at La Chapelle Bank. The winter biomass was between 0.1 and 0.4 $mg\,C\,m^{-3}$.

Seasonal variations in estimated mesozooplankton grazing rates ($mg\,C\,m^{-3}\,d^{-1}$) in Fig. 9 are very similar to the biomass data because they are derived from this parameter. However, the temperature dependence of the respiration and grazing estimates results in lower grazing per unit biomass in spring and higher specific grazing rate in summer. Grazing rate maximised in May with a value of 2.7 $mg\,C\,m^{-3}\,d^{-1}$, which contrasts with an estimated grazing rate of 0.6 $mg\,C\,m^{-3}\,d^{-1}$ in the same month at OMEX 2. Winter grazing rates are between 0.01 and 0.06 $mg\,C\,m^{-3}\,d^{-1}$.

However, in order to determine the grazing impact of mesozooplankton on phytoplankton, estimates are required of the total mesozooplankton that may migrate into the surface mixed layer to feed on phytoplankton and not merely the animals sampled by the CPR. The CPR samples at a fixed depth of ca. 10 m. Batten et al. (1999) have recently compared biomass estimates obtained by the CPR, with simultaneous depth profiles to 200 m of zooplankton abundance as sampled by the

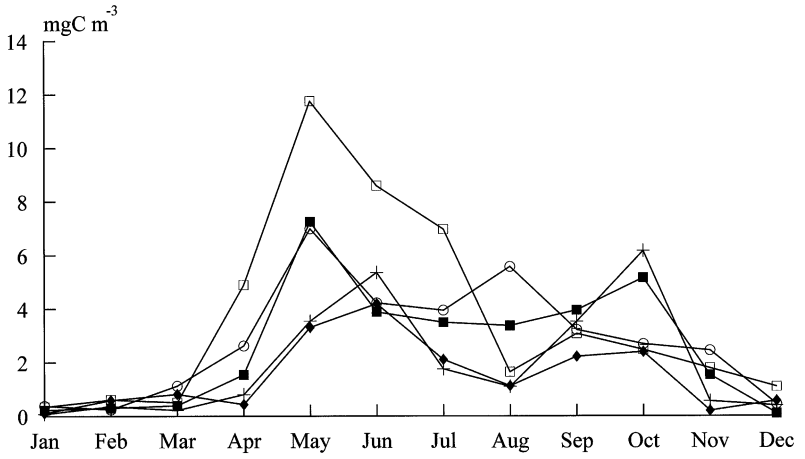

Fig. 8. Climatological-mean mesozooplankton biomass in the surface 10 m, estimated from the CPR survey data for 1963–1995. The regions are the Celtic Sea Shelf (□), the OMEX 1 region (■), OMEX 2 (+), OMEX 3 (♦), and La Chapelle Bank (○).

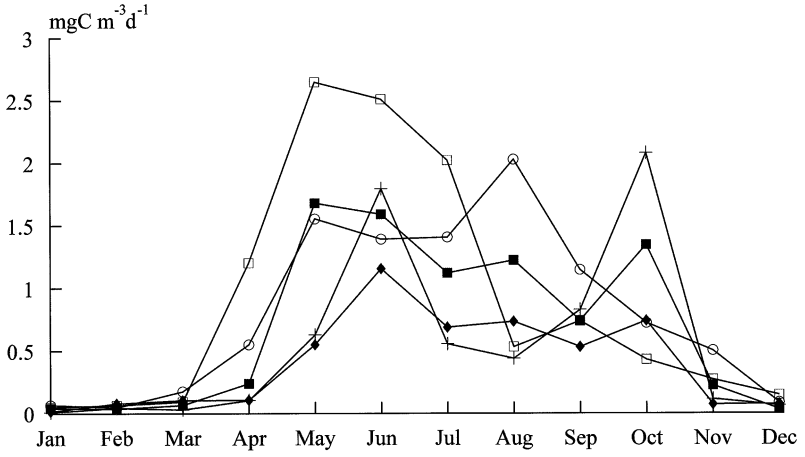

Fig. 9. Mesozooplankton grazing rates (mg C m^{-3} d^{-1}) for each month at the four stations on the Goban Spur and at La Chapelle Bank. The regions are the Celtic Sea Shelf (□), the OMEX 1 region (■), OMEX 2 (+), OMEX 3 (♦), and La Chapelle Bank (○).

Longhurst-Hardy Plankton Recorder. They found a close agreement between the biomass at 10 m and the mean biomass in the upper 200 m. In determining the grazing impact of mesozooplankton, the following is assumed: that the biomass sampled at 10 m by the CPR was equivalent to the mean integrated biomass in the surface 200 m; that all mesozooplankton in the surface 200 m were capable of migrating into the euphotic zone: that all mesozooplankton graze on phytoplankton cells; and that there was no significant vertical migration of animals from below 200 m into the surface mixed layer.

Table 5
Estimates of annual phytoplankton production and the annual carbon requirements of mesozooplankton, microzooplankton, and heterotrophic bacteria at each of the five regions of the Celtic Sea Shelf Break. All values are in $g C m^{-2} a^{-1}$

	Shelf	OMEX 1	OMEX 2	OMEX 3	La Chapelle Bank
Phytoplankton production	163	163	163	163	245
Mesozooplankton C requirement	83	53	43	31	64
Microzooplankton C requirement	(6)[a]	76	68	43	nd[b]
Bacterial C requirement	28	36	33	27	28
Unutilised phytoplankton production	(46)[a]	−2	19	62	(153)[b]

[a] Not an annual estimate since microzooplankton grazing estimates are only available for July.
[b] No microzooplankton data are available for La Chapelle Bank.

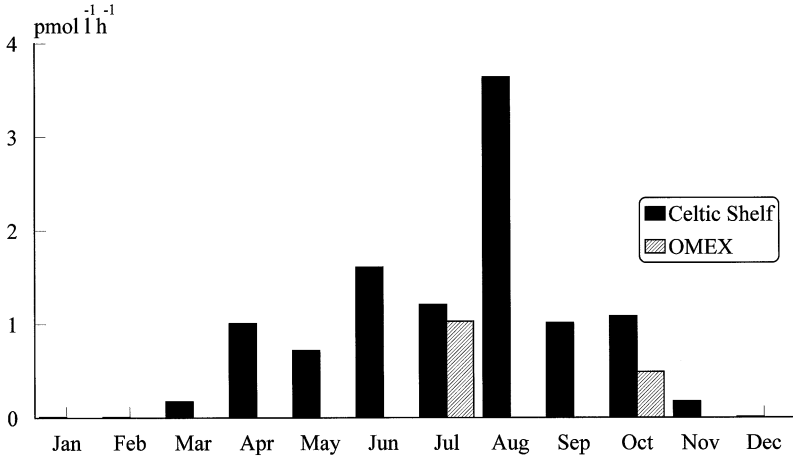

Fig. 10. Thymidine incorporation rates measured in the OMEX project compared with seasonal data published by Joint and Pomroy (1987).

Therefore, the total mesozooplankton grazing pressure was obtained by integrating the grazing rate ($mg C m^{-3} d^{-1}$) to 200 m (150 m in the case of the shelf region). Table 5 shows depth-integrated grazing ($mg C m^{-2} a^{-1}$) for each region, that is, the amount of carbon which is estimated to be ingested by mesozooplankton in the euphotic zone.

3.9. Bacterial activity

The final heterotrophic component of the food web measured during the OMEX project was bacterial activity but data were only obtained on two cruises. Therefore, seasonal estimates must rely on other data from the region. Joint and Pomroy (1987) published a seasonal estimate of bacterial production for the Celtic Sea shelf, based on the incorporation of ^{3}H-thymidine. Fig. 10 compares the thymidine incorporation rates measured in July 1993 and October 1995 with those

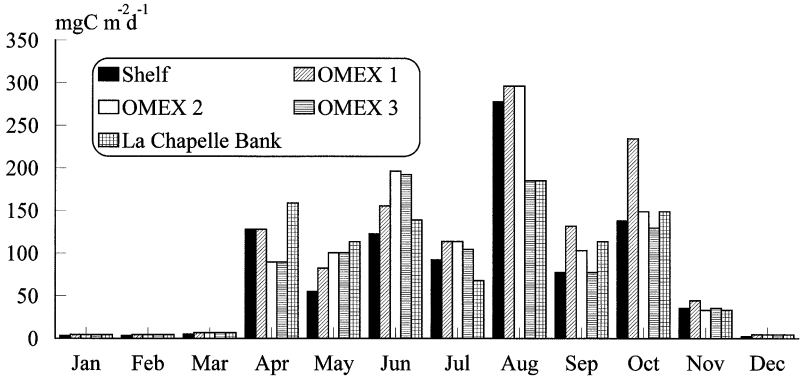

Fig. 11. Estimated carbon requirement by heterotrophic bacteria ($mg\,C\,m^{-2}\,d^{-1}$) in the surface mixed layer for each month.

of Joint and Pomroy (1987). The rates in July are comparable, but in October 1995 thymidine incorporation was approximately half that measured in 1982, perhaps reflecting the absence of an autumn phytoplankton bloom in 1995. Therefore, there is some justification for believing that the rates of bacterial activity measured by Joint and Pomroy (1987) are applicable to the Celtic Sea shelf margin.

Thymidine incorporation rates have been converted to depth-integrated production by assuming that a bacterial cell contains 20 fg C and that 2.65×10^{18} cells are produced per mol of thymidine incorporated; the production rate per m^3 is then multiplied by the depth of the surface mixed layer (Fig. 2). Bacteria are assumed to utilise organic matter with an efficiency of 50%. The estimated carbon requirement of the heterotrophic bacteria in the surface mixed layer in each month ($mg\,C\,m^{-2}\,d^{-1}$) is shown in Fig. 11. These conversion factors will tend to maximise the estimated carbon demand of the heterotrophic bacteria since they are at the upper end of the range of factors in the literature and may not be physiologically sound (Joint and Pomroy, 1987). Nevertheless, they are the factors that are in common use and are applied here because they allow comparison with similar recent work (Li et al., 1993).

4. Discussion

One aim of this paper is to determine how much of the carbon fixed by phytoplankton is mineralised in the surface mixed layer, hence providing an estimate of the potential supply of organic matter to the mid-water and benthos. Other papers in this volume describe the quantity of material collected in sediment traps on moorings at 1440 and 3260 m (Antia et al., 2001) and the respiration of benthic communities (van Weering et al., 2001). In order to produce carbon and nitrogen budgets for the Celtic Sea shelf break, estimates are required of carbon fixation and nitrogen assimilation into organic matter and the turnover of that carbon in the surface mixed layer. However, the approach taken in this paper, of using estimates for each calendar

month to construct budgets, has obvious limitations. It is difficult to make accurate seasonal determinations because biological activity varies temporally and spatially, on both short and long scales.

Most measurements in the OMEX Project were obtained over time scales of a few days. These have been averaged to give a typical daily value for the month of sampling, and this value has been applied throughout the calendar month. Therefore, temporal development within the month is not included. With data collection over the 3-y time scale of the OMEX 1 Project, there are inevitably differences between the rates measured in the same month in different years. No data are available for some months. Some estimates are based on only a small number of measurements in the OMEX project, but it has been possible to utilise data from other studies of the Celtic Sea shelf break or from adjacent regions, e.g., the estimates of phytoplankton and bacterioplankton production incorporate data collected in the Celtic Sea over more than a decade. In the case of mesozooplankton, the data are based on a very long time series of CPR data, so providing an excellent climatological mean biomass. Although this study does not consider interannual variability, this has been the subject of other papers, e.g., the variability in mesozooplankton biomass (Batten et al., 1999).

It has also not been possible to show differences in some rate measurements for each of the five regions discussed in this paper. Insufficient primary production measurements were made at sea in the four Goban Spur regions to show if any difference in phytoplankton production, but sufficient primary production estimates were made at La Chapelle Bank to compare the two regions. Similarly, the same bacterial production rate per m^3 has been applied to each region, but differences in the depth of the surface mixed layer result in different depth-integrated bacterial production estimates.

Some of the data obtained in the OMEX Project may have been obtained in years that were very different from the decadal average. For example, 1995 may have been anomalous, since there was no evidence of an autumn increase in phytoplankton production (Rees et al., 1999) in October 1995. Yet the long time-series phytoplankton colour index of the CPR (Fig. 3) indicates that an autumn bloom occurs frequently. Care is required in comparing the estimates made in this paper, which use October 1995 as representative of a typical October, with other models of the Goban Spur that might use a climatological mean. Nevertheless, in spite of the limitations of the data, the OMEX Project has provided a very extensive data set, and we present the following as the best attempt to date to budget carbon in the surface mixed-layer of the Celtic Sea shelf break.

4.1. Carbon budget for the euphotic zone at the Celtic Sea shelf edge

Since seasonal estimates have been made of primary production and grazing activity, it is possible to assess the balance between autotrophic and heterotrophic processes throughout the year and to consider which months show net autotrophy and which are heterotrophic. For the purposes of this budget, it is assumed that microzooplankton and mesozooplankton graze only on phytoplankton. It is also assumed that bacteria utilise directly the products of phytoplankton production and they are considered to be consumers of the carbon fixed by photosynthesis. This is a questionable assumption since the dissolved and particulate organic carbon that the bacteria utilise is generated by a number of different processes. However, this assumption, along with the conversion factors used in estimating bacterial production, will result in maximising the

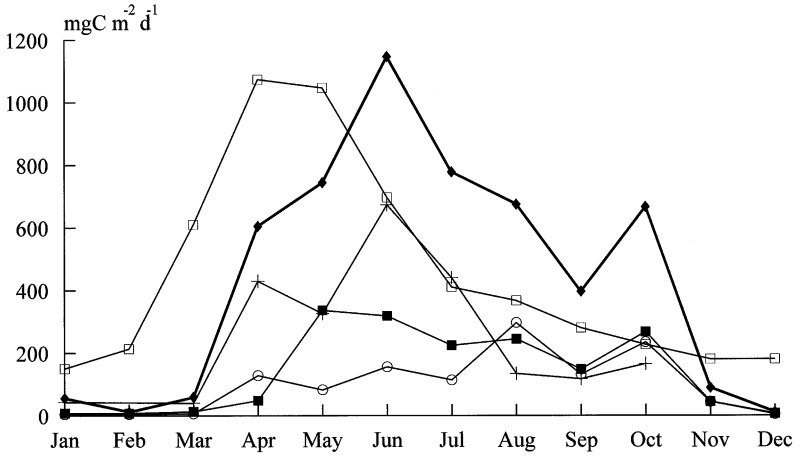

Fig. 12. Comparison of daily estimates for the OMEX 1 region of primary production (□) with mesozooplankton grazing (■) microzooplankton herbivory (+), carbon requirements of heterotrophic bacteria (○) and the sum of these three components to give the total carbon requirement of the heterotrophic community (◆).

demand of bacteria for phytoplankton production and hence minimising the quantity available for vertical flux.

The grazing demands of the mesozooplankton and microzooplankton, and the carbon demand of the bacterioplankton have been combined to give an estimate of "total grazing" on the carbon fixed each month by the phytoplankton assemblages. Fig. 12 shows the total carbon requirement of the heterotrophic community of the OMEX 1 region.

Microzooplankton grazing peaked in June with a carbon requirement of $\sim 0.7\,\mathrm{g\,C\,m^{-2}\,d^{-1}}$ but was low from August to October. Mesozooplankton grazing was relatively constant from May to October and was at a comparable rate to microzooplankton grazing in May. The carbon requirement of bacteria was highest in the autumn and was greater than the microzooplankton grazing rate. Again it is worth emphasising that the analysis performed here does not reflect the true complexity of the pelagic ecosystem since estimates of microzooplankton grazing on bacteria are not included. The total heterotrophic requirement (Fig. 12) at the OMEX 1 region was greater than the primary production rate from June to November, but there was a large excess of primary production in the spring from March to May. Calculations also have been made for the OMEX 2 and 3 regions, and these show similar results to OMEX 1, with heterotrophic consumption exceeding autotrophic production in summer and autumn. Since microzooplankton grazing data are not available for La Chapelle Bank and are sparse for the Shelf region, the total carbon requirement of the heterotrophic community in these regions cannot be assessed accurately.

An interesting feature of all regions is the major contribution made by mesozooplankton. This is in contrast to other studies such as the JGOFS North Atlantic Bloom Experiment. Morales et al. (1991) found that mesozooplankton is a small proportion of the plankton biomass and graze only a few percent of the daily phytoplankton production; Burkill et al. (1992) showed that microzooplankton was the major herbivore in the same region, accounting for between 39% and 115% of the daily primary production. In contrast, the data presented here suggest that

mesozooplankton grazing at the Celtic Sea shelf break is often greater than that of the microzooplankton, particularly in summer and autumn.

The high estimates of mesozooplankton grazing result from the assumption that the biomass measured by the CPR is representative of the whole of the upper 200 m (150 m on the shelf) and that all the mesozooplankton in that depth zone will migrate into the surface mixed layer to feed. The estimated mesozooplankton biomass in the 150-m water column at the shelf region in August is estimated to be 246 mg C m^{-2}. Joint and Williams (1985) sampled the Celtic Sea shelf and found the biomass of copepods to vary between 1097 and 1753 mg C m^{-2} over a 24-h period in August 1982. Therefore, the estimates of mesozooplankton biomass used in the present study are not overestimates and may even be underestimates. It is reasonable to conclude that, in this region, mesozooplankton grazing is very similar to microzooplankton herbivory.

Dissolved organic carbon (DOC) is an important constituent that has not been considered in this analysis but which could form a significant sink for carbon in the surface mixed layer. Data on DOC concentration were collected in January 1994 and June 1995 at OMEX 2, OMEX 3, and La Chapelle Bank. The mean DOC concentrations in winter, integrated over the upper 100 m, were 77 g C m^{-2} at OMEX 1 and 2, and 78 g C m^{-2} at OMEX 3. The DOC concentration in June showed little change at OMEX 1, with a concentration of 76 g C m^{-2}, but increased to 88 g C m^{-2} at OMEX 2 and 87 g C m^{-2} at La Chapelle Bank. Therefore, in the period between January and June, when primary production was about 113 g C m^{-2} (Table 3), DOC accumulated by about 10 g C m^{-2}. The organic carbon in the DOC presumably originates from phytoplankton production, but the organic compounds that comprise this DOC accumulation will result from a number of processes, including excretion by phytoplankton, microzooplankton and mesozooplankton and modification as a result of bacterial activity. At some time between June and January, the DOC concentration declines again but the rate of this decline is not known. Since the pathways of DOC production and breakdown are not known and have not been quantified, it is difficult to make a budget that includes DOC. Nevertheless, DOC in the upper 100 m in summer may be a sink for about 10% of the carbon fixed by phytoplankton.

4.2. Primary production not utilised in the surface mixed layer

The data for OMEX 1–3 have been combined in Fig. 13 to show the seasonal changes in the balance between phytoplankton production and heterotrophic consumption. Fig. 13 shows a consistent pattern in all three regions. In spring, phytoplankton production is greater than the sum of heterotrophic consumption and in April the excess of production over consumption was between 0.5 and 0.9 g C m^{-2} d^{-1}; that is, in spring all regions can be considered as autotrophic. The balance begins to change in June, with consumption at OMEX 1 and 2 being greater than production. Only OMEX 3, the region farthest to the west, continues to have marginally more primary production than heterotrophic consumption. In July, at OMEX 2, there is a deficit of $\sim$0.2 g C m^{-2} d^{-1} and from August to October, heterotrophic carbon requirement is consistently greater than phytoplankton production. At OMEX 1, the deficit is between 0.1 and 0.5 g C m^{-2} d^{-1} and at OMEX 3 between 0.1 and 0.2 g C m^{-2} d^{-1}.

Given the caveats that apply to this calculation, it appears that primary production at each region is significantly greater than the requirements of the heterotrophic community in the surface mixed layer for a period of $\sim$3 months in the spring. However, from July until October, there is

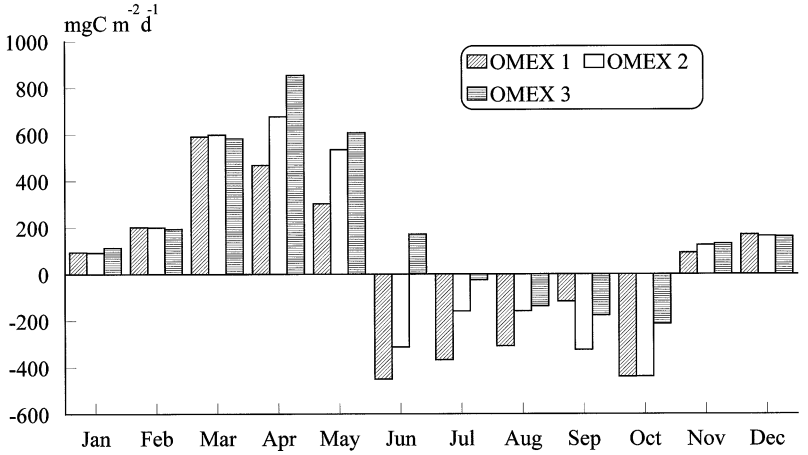

Fig. 13. Differences between phytoplankton production and the grazing requirement of the mesozooplankton, microzooplankton, and bacterioplankton for each month at the Goban Spur. Negative values indicate that the carbon requirement of the heterotrophic community exceeded phytoplankton production.

less phytoplankton production than the heterotrophic community requires. Table 5 summarises the estimates for each region. On an annual basis, most regions show net autotrophy, with an excess of primary production over heterotrophic requirement. OMEX 1 is close to balance, and the estimated annual primary production is approximately equivalent to the requirements of the heterotrophs. At OMEX 2 the excess of primary production over consumption is $19\,g\,C\,m^{-2}$ and at OMEX 3 it is $62\,g\,C\,m^{-2}\,a^{-1}$. Therefore, there appears to be a gradient of increasing excess phytoplankton production along the Goban Spur. Since the same phytoplankton production measurements have been applied to each region, this means a reduction in the grazing of microzooplankton and mesozooplankton at OMEX 2 and 3. At the Shelf region, where microzooplankton herbivory has not been included, the excess of production over consumption is no more than $46\,g\,C\,m^{-2}\,a^{-1}$. It appears that up to $\sim 60\,g\,C\,m^{-2}\,a^{-1}$ is not consumed in the surface mixed layer and therefore could potentially sediment into deeper water to be mineralised or transported to the sediment; that is, up to 38% of the primary production is not mineralised in the surface mixed layer.

4.3. Respiration in the surface mixed layer

The approach of determining herbivory rates used above gives a maximum estimate of the amount of phytoplankton carbon grazed by micro- and mesozooplankton since it assumed that zooplankton grazes only phytoplankton. The calculation ignores the fact that mesozooplankton also graze on microzooplankton and that microzooplankton graze on bacteria. However, the calculation does indicate the maximum amount of phytoplankton carbon that will be grazed within the surface mixed layer. An alternative calculation has been made by estimating the respiration of the heterotrophic assemblage. Table 6 shows the estimated respiration of mesozooplankton, microzooplankton, and heterotrophic bacteria at OMEX 1 and 3, which are compared with the daily primary production rates for each month; all data are expressed as

Table 6
Comparison of primary production and respiration estimates for each month at OMEX 1 and 3[a]

Month	Phytoplankton production (P) ($mg\,C\,m^{-2}\,d^{-1}$)	Mesozooplankton respiration (R_{meso}) ($mg\,C\,m^{-2}\,d^{-1}$)	Microzooplankton respiration (R_{micro}) ($mg\,C\,m^{-2}\,d^{-1}$)	Bacterial respiration (R_{bact}) ($mg\,C\,m^{-2}\,d^{-1}$)	R_{Tot} ($R_{meso}+R_{micro}+R_{bact}$) ($mg\,C\,m^{-2}\,d^{-1}$)	$P-R_{Tot}$ ($mg\,C\,m^{-2}\,d^{-1}$)
OMEX 1						
January	150	3.3	19.0	2.2	24.5	125.5
February	213	2.9	*30.0*	2.2	35.1	177.9
March	610	5.2	*50.0*	3.3	58.5	551.5
April	1073	19.1	227.3	64.0	310.4	762.6
May	1047	134.4	80.6	41.1	256.1	790.9
June	697	127.3	669.8	77.7	874.8	−177.8
July	410	89.7	772.1	56.9	918.7	−508.7
August	367	97.8	43.3	148.1	289.2	77.8
September	280	59.2	67.2	65.8	192.2	87.8
October	227	107.7	175.7	117.1	400.5	−173.5
November	180	17.8	*50.0*	22.1	89.9	90.1
December	180	2.6	*30.0*	2.2	34.8	145.2
OMEX 3						
January	150	1.3	19.9	2.2	23.4	126.6
February	213	6.3	30.0	2.2	38.5	174.5
March	610	8.3	50.0	3.3	61.6	548.4
April	1073	8.5	51.2	44.8	104.5	968.5
May	1047	44.0	375.0	50.3	469.3	577.7
June	697	92.5	56.6	96.1	245.2	451.8
July	410	55.0	216.9	52.3	324.2	85.8
August	367	58.7	84.0	92.6	235.3	131.7
September	280	42.4	218.0	38.7	299.1	−19.1
October	227	59.2	167.6	64.8	291.6	−64.6
November	180	5.6	*50.0*	17.7	73.3	106.7
December	180	5.9	*30.0*	2.2	38.1	141.9

[a] Values in italics were obtained by interpolation between months in which microzooplankton biomass was measured.

$mg\,C\,m^{-2}\,d^{-1}$ and are integrated to the base of the surface mixed layer, or to 200 m in the absence of a seasonal thermocline. The mesozooplankton estimate again assumes that animals migrate from the upper 200 m into the euphotic zone and that all ingestion takes place in the surface mixed layer. The mesozooplankton and bacterial respiration estimates are related to the grazing estimates (see Section 2), but the microzooplankton rates are independent, being derived from biomass estimates and not grazing experiments.

Like the grazing calculations, these estimates of respiration indicate an excess of autotrophy over heterotrophy within the surface mixed layer for much of the year. At OMEX 1, total respiration is greater than carbon fixation in June, July, and October. The annual respiration of the heterotrophic community at OMEX 1 is ca. $103\,g\,C\,m^{-2}$; therefore, ca. $60\,g\,C\,m^{-2}$ fixed by the

phytoplankton is not respired in the surface mixed layer and must be exported into deeper water. The community respiration at OMEX 3 is estimated to be only 66 g C m^{-2}, leaving ca. 97 g C m^{-2} for export. These calculations of respiratory rate suggest that between 37% and 60% of the carbon fixed is not respired in the surface mixed layer.

4.4. New production and excess primary production

The estimates of new production (Table 3) offer an independent confirmation of the potential vertical flux of carbon from the surface mixed-layer each year. Assuming that the nitrate that enters the surface mixed layer each year is balanced by the loss of all nitrogen species by sedimentation, the annual estimates of new production give an upper limit to the potential sedimentation of phytogenic material. Table 3 shows that the new production in the Celtic Sea is equivalent to $\sim$82 g C m^{-2} a^{-1}, which is half the estimated annual primary production. That is, over an annual cycle up to half the phytoplankton nitrogen (and hence the carbon production) may be exported out of the surface mixed layer to balance the supply of nitrate. This is consistent with the estimates obtained above comparing grazing pressure with primary production, that 16–60% of the primary production is not utilised by heterotrophs in the surface mixed layer.

The observed changes in nutrient conditions between winter and summer (when nitrate concentrations were below the limit of detection) can also be used to determine the maximum limit for new production that occurs during the spring bloom. Maximum nitrate concentrations at the Goban Spur measured in January 1994 ranged from 7.0 to 8.7 μmol N l^{-1}. The depth of the seasonal thermocline ranged from 40 to 60 m. If the initial assumption is made that there was no transport of nitrate across the thermocline, the total nitrate content of the water above the thermocline at the time of seasonal stratification would be 0.52 mol N m^{-2}. The Redfield ratio of 106C : 16N suggests that this quantity of nitrate could support the fixation of 3.46 mol C m^{-2} by phytoplankton—or 41.5 g C m^{-2}. This is consistent with the estimates in Table 3, which suggest that new production in the spring bloom (i.e., the sum of estimates for March–May) is 53.9 g C m^{-2}. However, this calculation does not account for transport of nitrate through the thermocline—a process that was not measured. An estimate of the approximate magnitude of this flux can be obtained from summer new production estimates. Throughout the summer months, nitrate concentrations were below the limit of detection, but new production, estimated from nitrate assimilation, was $\sim$3 g C m^{-2} $month^{-1}$. If it is assumed that this production results from the utilisation of nitrate transported into the euphotic zone and if nitrate was supplied at this rate through the spring bloom period, then an addition 9 g C m^{-2} over the period March–May would have been fixed as a consequence of nitrate utilisation–equivalent to the utilisation of 0.11 mol N m^{-2}. That is, a mass balance calculation of nitrate utilisation should include both the quantity of nitrate present at the onset of stratification (0.52 mol N m^{-2}) and the flux of nitrate through the thermocline (0.11 mol N m^{-2}). This should support primary production of 4.17 mol C m^{-2} (50.1 g C m^{-2}). That is, there is almost a perfect agreement between the new production estimated by ^{15}N-uptake experiments (53.9 g C m^{-2}) and from the change in nitrate concentration in the surface mixed layer (50.1 g C m^{-2}). From June to winter, new production is low and ammonium is the most important nitrogen source for the phytoplankton; this is consistent with the higher heterotrophic activity in this period, since with net heterotrophy, ammonium production should be maximised.

The change in nutrient concentrations also can quantify the potential importance of diatoms in the spring bloom. Winter concentrations of nitrate and silicate were $8.7\,\mu mol\,N\,l^{-1}$ and $2.8\,\mu mol\,Si\,l^{-1}$, respectively. Assuming that diatoms utilise nitrate and silicate with an atomic ratio of 1, that silicate was depleted in the spring bloom and that silicate was not rapidly recycled, diatoms would account for 32% of the new production in April and May.

4.5. Remote sensing estimates of new production

The question that has not been addressed so far in this paper is whether there was any measurable enhancement of phytoplankton production as a consequence of upwelling at the Goban Spur shelf break. The measurements of nitrate concentration in the surface water are equivocal and do not show any clear increases in nitrate concentration. However, the half-life of a nitrate signal in upwelled water is much shorter than that of temperature because of rapid assimilation of nitrate by phytoplankton. That is, it takes much longer for heat input to warm the cold water than it does for phytoplankton cells to assimilate nitrate in a well-illuminated oligotrophic environment such as the surface water of the Celtic Sea. Pingree (1984) has shown patches of high nitrate concentration associated with cooler water at the Celtic Sea shelf break south of the Goban Spur, but few of the measurements made in the OMEX project have shown increases in nitrate concentration. Therefore, what evidence is there that there is enhanced production at the shelf edge; is there any more than just a temperature signal? Rees et al. (1999) found increased *f*-ratio in the vicinity of the shelf break in October 1995. In September 1993, Elskens et al. (1997) found that nitrate concentrations were below the limit of detection at the Goban Spur, but concentrations increased along the continental shelf with concentrations up to $2\,\mu mol\,N\,l^{-1}$ in the vicinity of La Chapelle Bank. The *f*-ratio ranged from 0.29 to 0.70 and mirrored the nitrate distribution in the surface waters. The highest relative nitrate utilisation occurred at shelf stations that were characterised by intensive mixing and enhanced nitrate availability. These observations support the hypothesis that upwelling at the shelf break brings nutrients into the surface mixed layer, which are utilised by phytoplankton and enhance phytoplankton production.

Table 4 has shown that estimates of new production based on satellite remote sensing are comparable to those obtained by experiment; the satellite estimate is $46\,g\,C\,m^{-2}$ for the period April through September, and the comparable measured value is $57\,g\,C\,m^{-2}$. This gives credence to the estimates of new production obtained from satellite remote sensing. Since there is evidence for increased *f*-ratio at the shelf break and since satellite estimates of *f*-ratio are comparable to measured rates, the satellite data have been used to investigate the spatial variability in *f*-ratio. Fig. 6 suggests that the region of cool water along the shelf break translates into an area of elevated *f*-ratio.

4.6. Comparisons with sediment trap data

Finally, how does the material collected in the sediment traps compare with the monthly estimates of primary production in the euphotic zone? Microcrystalline barite, accounts for between 50% and 100% of the total barium in oceanic suspended matter (Dehairs et al., 1992). Material from the sediment traps was analysed for barium-barite and the data were used to

Table 7
Year-averaged POC and excess-Ba fluxes corrected for trapping efficiency; year-averaged excess-Ba fluxes corrected for trapping efficiency and advection; calculated export production

Site and depth of trap (m)	Trapping efficiency[a] (%)	F_{POC}[b] $g\,C\,m^{-2}\,a^{-1}$	F_{Baxs}[b] $\mu g\,cm^{-2}\,a^{-1}$	Advected fraction of F_{Baxs}	F_{Baxs}[c] $\mu g\,cm^{-2}\,a^{-1}$	ExP[d] $g\,C\,m^{-2}\,a^{-1}$
OMEX 2						
600	0.38	1.95	1.2	0.27	0.8	7.2
1050	0.85	2.10	1.2	0.47	0.7	4.6
OMEX 3						
580	0.34	1.79	1.8	0.08	1.7	20.0
1440	0.98	3.53	2.4	0.34	1.6	16.5
3260	1.05	2.14	1.9	0.33	1.3	10.6
4000	0.7	—	1.4	0	1.4	11.4

[a] Trapping efficiency as given in Antia et al. (1999).
[b] Observed POC and excess-Ba fluxes corrected for trapping efficiency.
[c] Observed excess-Ba flux corrected for trapping efficiency and advection of excess-Ba.
[d] Export production obtained using F_{Baxs} ($ExP = 22.7(F_{Baxs})^{1.504}Depth^{-0.139}$; (Dehairs et al., 2000).

calculate carbon export flux according to the rationale of Francois et al. (1995); the data were corrected for trapping efficiency (Antia et al., 2001) and for advection of Ba-barite. Furthermore, the Francois et al. method was adapted to account for the fact that in continental margin settings apparently a smaller amount of Ba-barite is produced per unit POC exported as compared to open ocean systems (Dehairs et al., 2000). Table 7 shows the carbon exported from the mixed surface layer, as deduced from the Ba-barite fluxes in the traps at OMEX sites 2 and 3. Values range from 11 to 20 $g\,C\,m^{-2}\,a^{-1}$ for OMEX 3 and from 4 to 7 $g\,C\,m^{-2}\,a^{-1}$ for OMEX 2. These results are significantly lower than the estimate of new production (80 $g\,C\,m^{-2}\,a^{-1}$) and suggest that not all of the exportable carbon estimated from new production is exported as a vertical POC flux; part may be exported out of the area by advective transport of either POC or DOC. Furthermore, the lower export values for OMEX 2 suggest that vertical export of carbon over the slope region proper was smaller than in the deep water stations further offshore.

5. Conclusions

A number of independent estimates suggest that a significant quantity of the carbon fixed by photosynthesis is not remineralised within the surface mixed layer. The calculations based on zooplankton herbivory indicate that, at the stations with the greatest water depth, up to 38% of photosynthetic carbon may be available for export. The respiration estimates suggest that heterotrophy within the surface mixed layer may be even less important and that between 37% and 60% of the primary production is not respired. Annual new production is estimated to be ca. 82 $g\,C\,m^{-2}$. If nitrate supply to the surface mixed layer is assumed to be balanced by losses of organic and inorganic nitrogen to deeper water, ca. 50% of the carbon fixed must be exported

from the seasonally stratified surface layer. This estimate of new production is supported by calculations of nitrate assimilation in the spring bloom, which indicate that nitrate supports production of ca. 54 g C m^{-2} in the spring bloom at the Goban Spur. Also approximately half of the annual production is by phytoplankton smaller than 5 μm, which have minimal sinking rates and are likely to be remineralised in the microbial loop in the surface mixed layer.

Therefore, the shelf margin of the Celtic sea is potentially a region of significant sedimentation of organic matter from the surface mixed layer.

Acknowledgements

The research was partially funded by the European Union in the framework of the MAST Programme, Project contract numbers MAS2-CT93-0069 and MAS3-CT96-0056 (Ocean Margin EXchange—OMEX).

References

Antia, A.N., von Bodungen, B., Peinert, R., 1999. Particle flux across the mid-European continental margin. Deep-Sea Research I 46, 1999–2024.

Antia, A.N., Maaβen, J., Herman, P., Voβ, M., Scholten, J., Groom, S., Miller, P., 2001. Spatial and temporal variability of particle flux at the N.W. European continental margin. Deep-Sea Research II 48, 3083–3106.

Barlow, R.G., Mantoura, R.F.C., Gough, M.A., Fileman, T.W., 1993. Pigment signatures of the phytoplankton composition in the northeastern Atlantic during the 1990 spring bloom. Deep-Sea Research II 40, 447–459.

Barlow, R.G., Mantoura, R.F.C., Peinert, R.D., Miller, A.E.J., Fileman, T.W., 1995. Distribution, sedimentation and fate of pigment biomarkers following thermal stratification in the Alboran Sea. Marine Ecology Progress Series 125, 279–291.

Barrie, A., Davies, J.E., Park, A.J., Workman, C.T., 1989. Continuous-flow stable isotope analysis for biologists. Spectroscopy 4, 42–52.

Batten, S.D., Hirst, A.G., Hunter, J., Lampitt, R.S., 1999. Mesozooplankton biomass in the Celtic Sea: a first approach to comparing and combining CPR and LHPR data. Journal of the Marine Biological Association of the UK 79, 179–181.

Biscaye, P.E., Flagg, C.N., Falkowski, P.G., 1994. The Shelf Edge Exchange Processes experiment, SEEP-II: An introduction to hypotheses, results and conclusions. Deep-Sea Research II 41, 231–252.

Burkill, P.H., Edwards, E.S., John, A.W.G., Sleigh, M.A., 1992. Microzooplankton and their herbivorous activity in the northeastern Atlantic Ocean. Deep-Sea Research II 40, 479–493.

Caron, D.A., Goldman, J.C., Fenchel, T., 1990. In: Capriulo, G.M. (Ed.), Ecology of Marine Protozoa.. Oxford University Press, New York, pp. 307–322.

Chin-Leo, G., Kirchman, D.L., 1988. Estimating bacterial production in marine waters from the simultaneous incorporation of thymidine and leucine. Applied and Environmental Microbiology 54, 1934–1939.

Colebrook, M.J., 1960. Continuous plankton records: methods of analysis, 1950–1959. Bulletin of Marine Ecology 5, 51–64.

Dehairs, F., Baeyens, W., Goeyens, L., 1992. Accumulation of suspended barite at mesopelagic depths and export production in the Southern Ocean. Science (NY) 258, 1332–1335.

Dehairs, F., Fagel, N., Antia, A.N., Peinert, R., Elskens, M., Goeyens, L., 2000. Export production in the Gulf of Biscay as estimated from barium-barite in settling material: a comparison with new production. Deep-Sea Research I 47, 583–601.

Dickson, R.R., Gurbatt, P.A., Narayana Pillai, V., 1980. Satellite evidence of enhanced upwelling along the European continental slope. Journal of Physical Oceanography 10, 813–819.

Dugdale, R.C., Goering, J.J., 1967. Uptake of new and regenerated forms of nitrogen in primary productivity. Limnology and Oceanography 12, 196–206.

Edwards, E.S., Burkill, P.H. Stelfox, C.E., 2001. Microzooplankton herbivory across the shelf-break at the Goban Spur, Celtic Sea from June 1993 to October 1995. Aquatic Microbial Ecology, submitted.

Elskens, M., Baeyens, W., Dehairs, F., Rees, A., Joint, I., Goeyens, L., 1999. Improved estimation of f-ratio in natural phytoplankton assemblages. Deep-Sea Research I 46, 1793–1808.

Elskens, M., Baeyens, W., Goeyens, L., 1997. Contribution of nitrate to the uptake of nitrogen by phytoplankton in an ocean margin environment. Hydrobiologia 353, 139–152.

Feldman, G.C., Kuring, N.A., Ng, C., Esaias, W.E., McClain, C.R., Elrod, J.A., 1989. Ocean color: Availability of the global data set. EOS 70, 634–641.

Francois, R., Honjo, S., Manganini, S.J., Ravizza, G.E., 1995. Biogenic barium fluxes to the deep sea: Implications for paleoproductivity reconstruction. Global Biogeochemical Cycles 9, 289–303.

Fiedler, R., Proksch, G., 1975. The determination of nitrogen-15 by emission mass spectrometry in biochemical analysis: a review. Analytica Chimica Acta 78, 1–62.

Fuhrman, J.A., Azam, F., 1982. Thymidine incorporation as a measure of heterotrophic bacterioplankton production in marine surface waters: evaluation and field results. Marine Biology 66, 109–120.

Gordon, H.R., Brown, J.W., Evans, R.H., 1988. Exact Rayleigh scattering calculations for use with the Nimbus-7 coastal zone color scanner. Applied Optics 27, 862–871.

Grasshoff, K., Ehrhardt, M., Kremling, K., 1983. Methods of Seawater Analysis, 2nd Edition. Verlag Chemie, Weinheim, p. 419.

Holm-Hansen, O., Lorenzen, C.J., Holmes, R.W., Strickland, J.D.H., 1965. Fluorometric determination of chlorophyll. Journal du Conseil International pour l'Exploration de la Mer 30, 3–15.

Huthnance, J.M., Coelho, H., Griffiths, C.R., Knight, P.J., Rees, A.P., Sinha, B., Vangriesheim, A., White, M., Chatwin, P.G., 2001. Physical structures, advection and mixing at Goban Spur. Deep-Sea Research II 48, 2979–3021.

Hydes, D.J., 1984. A manual of methods for continuous flow determination of ammonia, nitrate-nitrite, phosphate and silicate in sea water. Institute of Oceanographic Sciences, Report 177, p. 37.

Hydes, D.J., Le Gall, A.C., Miller, A.E.J., Brockmann, U., Raabe, T., Holley, S., Alvarez-Salgado, X., Antia, A., Balzer, W., Chou, L., Elskens, M., Helder, W., Joint, I., Orren, M., 2001. Supply and demand of nutrients and dissolved organic matter at and across the N.W. European shelf break in relation to hydrography and biogeochemical activity. Deep-Sea Research II 48, 3023–3047.

Ikeda, T., Motoda, S., 1978. Estimated zooplankton production and their ammonia excretion in the Kuroshio and adjacent seas. Fisheries Bulletin 76, 357–367.

IOC, Paris (France), 1994. Protocols for the Joint Global Ocean Flux Study (JGOFS) core measurements. Manual Guides IOC. Vol. 29, p. 126.

Joint, I., Groom, S.B., 2000. Estimation of phytoplankton production from space: current status and future potential of satellite remote sensing. Journal of Experimental Marine Biology and Ecology 250, 233–255.

Joint, I.R., Owens, N.J.P., Pomroy, A.J., 1986. The seasonal production of picoplankton and nanoplankton in the Celtic Sea. Marine Ecology Progress Series 28, 251–258.

Joint, I.R., Pomroy, A.J, 1987. Activity of heterotrophic bacteria in the euphotic zone of the Celtic Sea. Marine Ecology Progress Series 41, 155–165.

Joint, I.R., Williams, R., 1985. Demands of the herbivore community on phytoplankton production in the Celtic Sea in August. Marine Biology 87, 297–306.

Kirk, J.T.O., 1994. Light and Photosynthesis in Aquatic Ecosystems, 2nd Edition, Cambridge University Press, Cambridge, p. 509.

Koroleff, F., 1969. Direct determination of ammonia in natural waters as indophenol blue. ICES CM. 9, 19–22.

Landry, M.R., Hassett, R.P., 1982. Estimating the grazing impact of marine micro-zooplankton. Marine Biology 67, 283–288.

Li, W.K.W., Dickie, P.M., Harrison, W.G., Irwin, B.D., 1993. Biomass and production of bacteria and phytoplankton during the spring bloom in the western North Atlantic Ocean. Deep-Sea Research II 40, 307–327.

Morales, C.E., Bedo, A., Harris, R.P., Tranter, P.R.G., 1991. Grazing of copepod assemblages in the north-east Atlantic: The importance of the small fraction. Journal of Plankton Research 13, 455–472.

Owens, N.J.P., Rees, A.P., 1989. Determination of nitrogen-15 at submicrogram levels of nitrogen using automated continuous-flow isotope ratio mass spectrometry. Analyst 114, 1655–1657.

Parsons, T.R., Maita, Y., Lalli, C.M., 1984. A Manual of Chemical and Biological Methods for Sea-water Analysis. Pergamon, Oxford, p. 173.

Pingree, R.D., 1984. Some applications of remote sensing to studies in the Bay of Biscay, Celtic Sea and English Channel. In: Nihoul, J.C.J. (Ed.), Remote Sensing of Shelf Sea Hydrodynamics. Elsevier Amsterdam, pp. 287–315.

Pingree, R.D., Mardell, G.T., New, A.L., 1986. Propagation of internal tides from the upper slopes of the Bay of Biscay. Nature 321, 154–158.

Platt, T., Gallegos, C.L., Harrison, W.G., 1980. Photoinhibition of photosynthesis in natural assemblages of marine phytoplankton. Journal of Marine Science 38, 687–701.

Rees, A.P., Joint, I., Donald, K.M., 1999. Early spring bloom phytoplankton-nutrient dynamics at the Celtic Sea Shelf Break. Deep-Sea Research I 46, 483–510.

Sathyendranath, S., Platt, T., Horne, E.P.W., Harrison, W.G., Ulloa, O., Outerbridge, R., Hoepffner, N., 1991. Estimation of new production in the ocean by compound remote sensing. Nature 353, 129–133.

Schneider, G., 1989. Carbon and nitrogen content of marine zooplankton dry material: A short review. Plankton Newsletter 11, 4–7.

Simon, M., Azam, F., 1989. Protein content and protein synthesis rates of planktonic marine bacteria. Marine Ecology Progress Series 51, 201–213.

Vazquez, J., Hamilton, M., van Tran, A., Sumagaysay, R.M., 1994. JPL physical oceanography DAAC reprocesses ten years of sea-surface temperature measurements from NOAA AVHRR. The Earth Observer 6, 16–17.

Walsh, J.J., Biscaye, P.E., Csanadt, G.T., 1988. The 1983–1984 Shelf Edge Exchange Process (SEEP)-I experiment: hypotheses and highlights. Continental Shelf Research 8, 435–456.

Walsh, J.J., Rowe, G.T., Iverson, R.L., McRoy, C.P., 1981. Biological export of shelf carbon is a sink of the global CO_2 cycle. Nature 291, 196–201.

van Weering, T.C.E., Hall, I.R., de Stigter, H.C., McCave, I.N., Thomsen, L., 1998. Recent sediments, sediment accumulation and carbon burial at Goban Spur, NW European Continental Margin (47–50°N). Progress in Oceanography 42, 5–35.

van Weering, Tj.C.E., De Stigter, H.C., Balzer, W., Epping, E.H.G., Graf, G., Hall, I.R., Helder, W., Khripounoff, A., Lohse, L., McCave, I.N., Thomsen, L., Vangriesheim, A., 2001. Benthic dynamics and carbon fluxes on the NW European continental margin. Deep-Sea Research II 48, 3191–3221.